REPUBLIC OF TURKEY
ACIBADEM MEHMET ALI AYDINLAR UNIVERSITY
INSTITUTE OF NATURAL AND APPLIED SCIENCES

PERFORMANCE COMPARISON OF FNIRS SIGNAL PREPROCESSING APPROACHES WITH AND WITHOUT SHORT CHANNEL REGRESSION

Alper GÜVEN
DEPARTMENT OF BIOMEDICAL ENGINEERING
MASTER'S THESIS

SUPERVISOR
Assoc. Prof. Sinem Burcu ERDOĞAN

ISTANBUL - 2023

DECLARATION

I declare that the information reported in this thesis is the result of my own work, except where explicitly stated otherwise in the text. I am fully aware of all the ethical rules and there are not any violations of copyright and any kind of patent.

25.08.2023

Alper Güven

ACKNOWLEDGEMENT

I would like to express my sincere gratitude to my supervisor, Associate Professor Sinem Burcu Erdoğan, for her unwavering guidance, invaluable insights, and continuous support throughout the process of completing this master's thesis. Her expertise, dedication, and encouragement have been instrumental in shaping the direction of my research and enhancing the quality of this work. I am truly fortunate to have had her as my supervisor, and I am deeply appreciative of her contributions to my academic journey.

And also, I am profoundly grateful to my parents, whose boundless love, unwavering encouragement, and unwavering belief in my potential have been the driving force behind my academic accomplishments. Their constant support, sacrifices, and guidance have been the cornerstone of my journey, motivating me to overcome challenges and pursue my aspirations. Their unyielding faith in my abilities has been a constant source of strength, and I am deeply thankful for their endless encouragement and the values they instilled in me. This achievement would not have been possible without their immeasurable contributions, and I dedicate this thesis to them with heartfelt appreciation.

TABLE OF CONTENTS

LIST OF ABBREVIATIONS

FNIRS Functional Near Infrared Spectroscopy

FMRI Functional Magnetic Resonance Imaging

NIR Near Infrared

Cm Centimeter

HBO Oxyhemoglobin

HBR Deoxyhemoglobin

MRI Magnetic Resonance Imaging

PET Positron Emission Tomography

EEG Electroencephalography

SPECT Single-Photon Emission Computed Tomography

DTI Diffusion Tensor Imaging

MEG Magnetoencephalography

CT Computed Tomography

ERPs Event-related Potentials

SQUIDs Superconducting Quantum Interference Devices

MIT Massachusetts Institute of Technology

BCI Brain-computer Interface

FDG Fluorodeoxyglucose

CW Continuous Wave

MBLL Modified Beer-Lambert Law

HBO2 Oxygenated hemoglobin

LDs Laser Diodes

SNR Signal-to-noise Ratio

OD Optical Density

LEDs Light Emitting Diodes

CV Coefficient of Variation

PCA Principal Component Analysis

ICA Independent Component Analysis

FORs Functional Optical Responses

FFT Fast Fourier Transform

CBSI Correlation-based Signal Improvement

GLM General Linear Model

APD Avalanche Photodiode

DPF Differential Pathlength Factor

SSR Short Separation Regression

SS Short Separation

SG Savitzky-Golay

MCSG Motion Correction Spline Savitzky-Golay

TTP Time to Peak

CNR Contrast-to-noise Ratio

BP Bandpass

ROI Regions of Interest

LIST OF FIGURES

LIST OF TABLES

SUMMARY

Functional Near-Infrared Spectroscopy (fNIRS) has emerged as a valuable non-invasive neuroimaging technique that holds immense potential for unraveling the mysteries of human brain function and cognition. By measuring the changes in hemodynamic responses, particularly the fluctuations in oxyhemoglobin and deoxyhemoglobin concentrations, fNIRS offers a window into the dynamic neural activity underlying cognitive processes. However, the accurate extraction of these subtle hemodynamic signals is often impeded by various confounding factors, among which short channel separation and noise contamination prominently feature. Short channels, or optodes placed at a minimal distance from the sources and detectors on the scalp, are particularly susceptible to capturing extracranial physiological activity, contaminating the recorded signals. Moreover, environmental and physiological noise sources further obfuscate the signal of interest. To address these challenges, researchers have been ardently developing and refining noise reduction techniques, ranging from traditional filtering methods to sophisticated machine learning algorithms. These techniques play a pivotal role in enhancing the quality of fNIRS data, ultimately advancing our understanding of human brain function and paving the way for more robust and insightful neuroimaging studies. The aim of this study is to find the best noise reduction technique by comparing 10 fNIRS processing methods in the dataset collected with audio tasks using short channel separation.

Keywords: Functional near-infrared spectroscopy, Processing, Noise reduction, Motion correction, Contrast to noise ratio, Bandpass filtering, Audio, Optical Density, Modified Beer-Lambert law, Short channel separation

ÖZET

İşlevsel Yakın Kızılötesi Spektroskopi (İYKAS), insan beyninin işlevini ve bilişsel süreçlerin gizemlerini çözmede büyük potansiyele sahip önemli bir invaziv olmayan nörogörüntüleme tekniği olarak ortaya çıkmıştır. Oksihemoglobin ve deoksihemoglobin konsantrasyonlarındaki değişiklikleri ölçerek, özellikle dinamik sinirsel aktivitenin bilişsel süreçlerin temelindeki dalgalanmaları, İYKAS, bize bilişsel süreçlerin temelindeki dinamik sinirsel aktiviteye bir pencere sunar. Bununla birlikte, bu ince hemodinamik sinyallerin doğru bir şekilde çıkarılması, genellikle çeşitli karıştırıcı faktörler tarafından engellenir, bunlar arasında özellikle kısa kanal ayrımı ve gürültü kirliliği yer alır. Kısa kanallar, kaynak ve detektörlerin kafa derisine minimal bir mesafede yerleştirildiği optotlardır ve özellikle ekran dışı fizyolojik aktiviteyi yakalama eğilimindedir, bu da kaydedilen sinyalleri kirletir. Dahası, çevresel ve fizyolojik gürültü kaynakları ilgi çekici sinyali daha da belirsizleştirir. Bu zorlukların üstesinden gelmek için araştırmacılar, geleneksel filtreleme yöntemlerinden sofistike makine öğrenimi algoritmalarına kadar uzanan gürültü azaltma tekniklerini özenle geliştirip iyileştirmektedirler. Bu teknikler, İYKAS verilerinin kalitesini artırmada kilit bir rol oynamakta olup, nihayetinde insan beyin işlevinin anlayışımızı ilerletmekte ve daha sağlam ve içgörülü nörogörüntüleme çalışmalarının yolunu açmaktadır. Bu çalışmanın amacı, kısa kanal ayrımı kullanılarak sesli görevlerle elde edilen veri setinde 10 İYKAS işleme yöntemini karşılaştırarak en iyi gürültü azaltma tekniğini bulmaktır.

Anahtar Kelimeler: İşlevsel yakın kızılaltı spektroskopi, İşleme, Gürültü azaltma, Hareket düzeltme, Kontrast-gürültü oranı, Bant geçiren filtreleme, Sesli, Optik Yoğunluk, Modifiye Edilmiş Beer-Lambert yasası, Kısa kanal ayrımı

1. INTRODUCTION

Modern human brain research has experienced an increasing interest in the use of a novel non-invasive optical imaging technique known as functional near infrared spectroscopy (fNIRS) for neuroscientific research in the last couple of decades. As a proxy for neural activity, fNIRS is a wearable optical neuroimaging technology that can simply assess variations in cortical oxygenation dynamics (1).

FNIRS has a significant promise as an imaging modality for clinical research, basic and applied research because of its low cost, simplicity of use at the bedside, and compatibility with other complementary electrophysiological approaches. It can also be used in a variety of applications, including neurodevelopmental research where it has significant potential to replace and/or assist neurophysiological data obtained from functional magnetic resonance imaging (fMRI) (2).

FNIRS systems utilize near infrared (NIR) light directed at the scalp to monitor changes in regional cerebral oxygenation resulting from neuronal activation. However, before reaching the cortical tissue, the NIR light must pass through the scalp, skull, and cerebrospinal fluid compartments. The human brain tissue is complex, being anisotropic and inhomogeneous across its different layers, which adds intricacy to how the NIR light interacts with it (3).

A continuous wave fNIRS device functions by continuously exposing the brain to a fixed intensity of incident light while simultaneously detecting changes in the intensity of the reflected light, which allows for the assessment of brain activity. This process involves the penetration of several layers of brain tissue, including the scalp, skull, cerebrospinal fluid, gray matter, and white matter, by the emitted light from the sensors placed on the subject's scalp. Throughout this penetration, some photons undergo deflection or scattering, while others manage to pass through the layers and are captured by a detector located on the scalp, typically positioned around 0.5 to 5.5 cm away from the emitters.

The resulting changes in intensity of the detected photons are then subjected to the modified Beer-Lambert formula to calculate the corresponding alterations in the concentrations of oxyhemoglobin (HbO) and deoxyhemoglobin (HbR). This allows researchers to infer and monitor changes in brain oxygenation levels, serving as a valuable tool in studying brain function and neural activity (4).

2. BACKGROUND

2.1. Brain Imaging Techniques

Brain imaging techniques are invaluable tools used to study the intricate workings of the human brain. These non-invasive methods allow researchers and medical professionals to visualize brain structures, functions, and abnormalities, contributing to our understanding of cognition, behavior, and neurological disorders.

Magnetic Resonance Imaging (MRI) is one of the most widely used brain imaging techniques, which employs powerful magnets and radio waves to generate detailed images of the brain's soft tissues, providing high-resolution anatomical information. Complementing MRI, functional Magnetic Resonance Imaging (fMRI) measures changes in blood flow, indicating brain activity during various tasks and revealing functional connectivity patterns.

Positron Emission Tomography (PET) is another powerful tool that involves the injection of a radioactive tracer, allowing the visualization of metabolic processes and neurochemical activities in the brain.

Single-Photon Emission Computed Tomography (SPECT) is similar to PET but uses a different type of tracer and is more widely available.

Diffusion Tensor Imaging (DTI) focuses on the brain's white matter tracts, enabling researchers to study the connectivity and communication between different brain regions.

Electroencephalography (EEG) and Magnetoencephalography (MEG) measure electrical and magnetic activity in the brain, respectively, with high temporal resolution, aiding the study of neural oscillations and brain rhythms.

Lastly, Computed Tomography (CT) scans use X-rays to create cross-sectional images of the brain, often used in emergency situations due to its rapid results.

Each brain imaging technique possesses unique strengths and limitations, collectively enhancing our knowledge of the brain's complexity and advancing medical diagnoses and treatments for various neurological conditions.

Electroencephalography (EEG)

Electroencephalography (EEG) is a valuable neuroimaging technique that records and measures the electrical activity of the brain through the use of electrodes placed on the scalp. The history of EEG dates back to the late 19th century when the British physician Richard Caton first observed electrical signals in the brains of animals. However, it was not until 1924 when German psychiatrist Hans Berger made a groundbreaking discovery by successfully recording human brain waves using his electroencephalograph. His pioneering work opened up new avenues for understanding the brain's electrical activity and led to the term “electroencephalogram." (5).

Over the years, EEG technology has significantly evolved, becoming more sophisticated and accessible. Early EEG machines were limited by their cumbersome nature and low signal resolution, but advancements in electronics and computing have dramatically improved the quality and efficiency of EEG recordings (6). Modern EEG systems consist of multiple electrodes placed strategically across the scalp to capture brain activity from different brain regions simultaneously.

EEG is widely used in various fields, including neuroscience, clinical medicine, and psychology. In neuroscience research, EEG helps researchers investigate brain functions related to cognition, attention, memory, and sleep. Moreover, it plays a pivotal role in diagnosing and monitoring neurological disorders such as epilepsy, sleep disorders, and brain injuries. The characteristic EEG patterns associated with different conditions aid in accurate diagnosis and inform treatment strategies (6).

One of the key advantages of EEG is its exceptional temporal resolution, allowing researchers to observe brain activity in real-time. This capability is particularly useful in studying event-related potentials (ERPs), which are specific brain responses elicited by external stimuli or internal mental processes. The ability to precisely time neural events makes EEG an essential tool for studying cognitive processes with high temporal precision (7).

Despite its many strengths, EEG also has limitations. Its spatial resolution is relatively low compared to other brain imaging techniques like fMRI or MRI. The signals measured by EEG are attenuated as they pass through the skull and scalp,

making it challenging to precisely locate the source of activity within the brain. To address this limitation, researchers often combine EEG with other neuroimaging modalities to gain a more comprehensive understanding of brain function and connectivity (7).

In recent years, EEG technology has seen further advancements with the development of wearable EEG devices, making it possible to conduct studies outside the laboratory setting. These portable EEG systems have opened up new opportunities for monitoring brain activity during real-world tasks and enhancing brain-computer interface (BCI) applications.

Overall, EEG remains a crucial and versatile tool in neuroscience and clinical practice, continuously contributing to our understanding of brain function and providing valuable insights into the complexities of the human mind. As technology continues to progress, EEG is likely to play an increasingly significant role in diagnosing and treating neurological conditions and exploring the mysteries of the brain.

Functional Magnetic Resonance Imaging (fMRI)

Functional Magnetic Resonance Imaging (fMRI) is a powerful brain imaging technique that allows researchers and clinicians to non-invasively visualize and measure brain activity based on changes in blood flow. The roots of fMRI can be traced back to the development of MRI technology in the early 1970s. MRI, which stands for Magnetic Resonance Imaging, was initially used for anatomical imaging and provided detailed images of the brain's structure without the need for ionizing radiation. It was a revolutionary advancement in medical imaging, but it wasn't until the early 1990s that fMRI emerged as a groundbreaking extension of MRI.

The key breakthrough in fMRI came with the recognition that changes in blood oxygenation levels are tightly linked to neural activity. This relationship, known as the "hemodynamic response," forms the basis of fMRI. When a specific region of the brain becomes more active, it requires more oxygen to support the increased metabolic demand. In response, blood flow to that area increases to deliver oxygen-rich blood, resulting in a detectable change in the MRI signal.

The first fMRI experiments were conducted by three research groups independently in 1991. Seiji Ogawa, Ken Kwong, and Kamil Uğurbil, along with their teams, demonstrated the feasibility of fMRI in mapping brain activity during simple tasks. Their seminal studies set the stage for fMRI's rapid expansion in neuroscience and cognitive research (8).

Since its inception, fMRI has evolved significantly, leading to improved image quality, increased spatial resolution, and more sophisticated data analysis techniques. With the advent of high-field MRI scanners and advanced data processing methods, researchers can now capture detailed brain activity patterns with unprecedented precision.

fMRI has become an essential tool in cognitive neuroscience, allowing researchers to explore the functional organization of the human brain. By presenting participants with various stimuli or tasks, scientists can study how different brain regions respond and interact during specific cognitive processes. For instance, fMRI studies have unveiled brain networks associated with attention, memory, language, emotion, and decision-making (7).

In the clinical realm, fMRI has found applications in pre-surgical planning, particularly in cases involving brain tumors or epilepsy. By identifying critical functional regions in individual patients, surgeons can avoid damaging vital areas and reduce the risk of post-surgical deficits. Additionally, fMRI has been utilized to investigate neurological and psychiatric disorders, providing insights into their underlying neural mechanisms. While fMRI offers exceptional spatial resolution, it has limitations. The hemodynamic response has a relatively slow time course, which restricts the temporal resolution of fMRI compared to other brain imaging techniques like EEG. Furthermore, fMRI requires participants to lie still within the confined space of an MRI scanner, potentially limiting the examination of certain behaviors or conditions that may be more naturalistic (7).

In conclusion, fMRI has revolutionized brain research and clinical neuroscience by enabling non-invasive investigation of brain function. Its ability to map brain activity and connectivity has provided unprecedented insights into the human mind and opened up new avenues for understanding neurological disorders. As technology

continues to advance, fMRI is expected to remain a cornerstone in brain research, leading to even more sophisticated applications and furthering our understanding of the complexities of the human brain.

Magnetoencephalography (MEG)

Magnetoencephalography (MEG) is a unique and valuable brain imaging technique that measures the magnetic fields generated by neuronal activity in the brain. The history of MEG can be traced back to the 1960s when researchers first observed the magnetic signals produced by the human brain. However, it was not until the 1970s that MEG began to gain recognition as a practical method for studying brain activity. The breakthrough came with the development of superconducting quantum interference devices (SQUIDs), which are highly sensitive to magnetic fields (9) These devices allowed for more accurate and precise measurement of the weak magnetic signals generated by the brain's neural currents. In 1968, David Cohen and his team at the Massachusetts Institute of Technology (MIT) built the first whole-head MEG system, which paved the way for the modern MEG technology we use today (10).

MEG offers several advantages over other brain imaging techniques. One of its key strengths is its exceptional temporal resolution, providing precise measurements of neural activity on a millisecond timescale. This ability is particularly valuable for studying the rapid dynamics of brain processes, such as those involved in perception, language, and motor control. Additionally, MEG has excellent spatial resolution, allowing researchers to pinpoint the location of neural activity within the brain with high accuracy.

MEG has become a vital tool in neuroscience and cognitive research. It has helped reveal fundamental brain mechanisms involved in sensory perception, memory, attention, and language processing. MEG studies have contributed to our understanding of brain networks and how different regions interact during various cognitive tasks. Moreover, MEG is instrumental in investigating abnormal brain activity and functional connectivity patterns in neurological disorders, such as epilepsy and autism spectrum disorders (11).

MEG's non-invasive nature and high temporal and spatial resolution have also made it an important tool in brain-computer interface (BCI) research. BCI systems

enable direct communication between the brain and external devices, holding great promise for assisting individuals with motor disabilities or communication impairments.

Despite its advantages, MEG does have some limitations. The main challenge lies in its susceptibility to magnetic interference from the environment and surrounding electronics. To address this, MEG labs are specially shielded to minimize external magnetic fields' impact on measurements. Additionally, MEG signals are weaker than electrical signals measured by EEG, which can limit its sensitivity to deep brain structures (12).

In recent years, MEG technology has continued to advance. The development of novel sensor arrays, improved data analysis techniques, and the integration of MEG with other neuroimaging modalities, such as fMRI and EEG, have further enhanced its capabilities. Additionally, advancements in software and computational methods have facilitated the extraction of more detailed information from MEG data, expanding its applications in both research and clinical settings.

In conclusion, MEG is a powerful and versatile brain imaging technique that provides unique insights into the dynamics of neural activity in the human brain. Its ability to capture millisecond-scale brain processes with high spatial accuracy has been instrumental in advancing our understanding of brain function and dysfunction. As technology continues to progress, MEG is likely to play an increasingly significant role in neuroscience, offering new opportunities to explore the complexities of the brain and improve our knowledge of the human mind.

Positron Emission Tomography (PET)

Positron Emission Tomography (PET) is a powerful and versatile brain imaging technique that provides valuable insights into brain function and metabolism. The history of PET dates back to the 1950s when scientists first began exploring the use of positron-emitting isotopes in medical imaging. However, it was not until the 1970s that PET technology started to be used for brain imaging. The breakthrough came with the development of cyclotrons, which allowed for the production of short-lived positron-emitting isotopes. In 1976, Michael E. Phelps and Edward Hoffman successfully demonstrated the application of PET to measure brain activity using the

radiotracer 18F-fluorodeoxyglucose (FDG), a glucose analogue that reveals regional brain glucose metabolism (13).

PET is particularly valuable in brain imaging due to its ability to visualize and quantify metabolic processes and neurochemical activities in vivo. By using specific radiotracers, PET can measure various aspects of brain function, including glucose metabolism, regional blood flow, receptor density, and neurotransmitter binding. For example, FDG-PET is widely used to assess brain glucose metabolism, which is an essential marker of brain activity and energy utilization. PET studies with radiotracers targeting neurotransmitter systems, such as dopamine and serotonin, have provided insights into the neurochemical basis of various neuropsychiatric disorders.

In neuroscience research, PET has played a critical role in investigating brain function and mapping neural networks associated with various cognitive processes. It has been employed to study memory, attention, language, emotion, and decision-making. PET studies have also contributed to our understanding of brain plasticity, showing how the brain reorganizes and adapts in response to learning, injury, or disease. In clinical medicine, PET has become an indispensable tool in the diagnosis, staging, and treatment evaluation of neurological disorders. For instance, in the early diagnosis of Alzheimer's disease, PET imaging with radiotracers targeting amyloid plaques or tau tangles allows for the detection of characteristic pathological changes before significant cognitive decline occurs.

PET is also widely used in the evaluation of epilepsy, brain tumors, and movement disorders, providing crucial information for surgical planning and patient management.

Moreover, PET is utilized in drug development and pharmacological research. Preclinical PET studies in animal models help researchers understand drug pharmacokinetics and pharmacodynamics, while clinical PET trials enable the evaluation of drug effects on specific brain targets, receptor occupancy, and drug distribution in the brain.

While PET offers exceptional molecular and functional information, it does have some limitations. The use of radioactive isotopes requires specialized facilities and strict radiation safety protocols. Additionally, the short half-life of some radiotracers

limits their availability and necessitates on-site production with cyclotrons or other accelerators(13).

Recent advancements in PET technology, such as the development of hybrid NeuroPET/CT and PET/MRI systems, have further expanded its capabilities. The integration of PET with other imaging modalities allows for more comprehensive assessments of brain structure, function, and metabolism (13).

In conclusion, PET is a versatile and essential tool in brain imaging, providing valuable information about brain function, metabolism, and neurochemistry. Its applications in neuroscience, clinical medicine, and drug development have significantly contributed to our understanding of the brain and its role in health and disease. As PET technology continues to evolve, it is likely to remain a critical component of brain research and clinical practice, offering new opportunities to advance our knowledge and improve patient care.

2.2. New Technique For Brain Imaging: Functional Near-Infrared Spectroscopy (FNIRS)

Functional Near-Infrared Spectroscopy (fNIRS) is a novel brain imaging technique gaining popularity in functional neuroimaging research. It non-invasively examines changes in brain oxygenation levels through transillumination. Over the past two decades, interest in fNIRS has grown due to its real-time monitoring capabilities, cost-effectiveness, radiation-free nature, portability, and patient-friendly characteristics. It finds applications in brain-computer interface and functional neuroimaging research, as well as in clinical contexts like Alzheimer's disease, schizophrenia, dyslexia, Parkinson's disease, childhood disorders, post-neurosurgery dysfunction, attention, functional connectivity, and more. This versatile technique offers potential for diagnosis and assists in clinical approaches (14).

The roots of fNIRS can be traced back to the early 1970s when researchers first explored the application of near-infrared light to study biological tissues. However, it was not until the 1990s that fNIRS started to gain popularity as a brain imaging tool. The breakthrough came with the development of better light sources, detectors, and data analysis methods. In the past, fNIRS was mainly used in the field of physiology

to assess tissue oxygenation and blood flow. But its application to brain imaging expanded rapidly due to its non-invasive nature, portability, and affordability.

The development of in vivo Near-Infrared Spectroscopy (NIRS) was pioneered by Frans Jöbsis, who discovered its potential for non-invasive detection of hemoglobin oxygenation in the brain using transillumination spectroscopy in 1977. Marco Ferrari also made significant contributions, utilizing prototype NIRS instruments to measure brain oxygenation in experimental animal models and human adults in the 1980s. David Delpy further advanced NIRS by developing quantitative measurements of oxygenation and hemodynamic parameters in sick newborn infants. Over the years, various companies collaborated with research institutions to develop NIRS prototypes, leading to the creation of the first commercial NIRS system, the NIRO-1000, in 1989 by Hamamatsu Photonics. From 1980 to 1995, nine companies joined the effort to develop NIRS technology (15).

Near-Infrared Spectroscopy (NIRS) relies on the transparency of human tissues to light in the NIR spectral range (650–1000 nm). NIR light can be absorbed or scattered in tissues, but its dominant mode of transport is scattering, making it capable of penetrating human tissues. Hemoglobin, present in small vessels of the microcirculation, causes the main attenuation of NIR light in tissues, and larger blood vessels have minimal impact on NIRS measurements. NIRS uses safe laser diode and/or light-emitting diode light sources along with flexible fiber optics for delivering and detecting NIR light in tissues. This non-invasive technique permits monitoring of physiological parameters, including oxygenated and deoxygenated hemoglobin levels and cerebral blood volume. It offers spatial sensitivity to brain activity despite the complexity of light scattering in tissues (14).

Functional Near-Infrared Spectroscopy (fNIRS) in the form of Continuous Wave (CW fNIRS) highlighting its relatively simple setup and practical applications. To conduct CW fNIRS measurements, a Near-Infrared (NIR) light source is activated, and the emitted light is directed into the scalp. The light that re-emerges from the tissue a few centimeters away is then measured to gather valuable data. The simplicity of CW fNIRS setups allows for specialization in wearable, miniaturized, and wireless applications, making it a versatile tool for various research and clinical scenarios.

Additionally, the cost-effectiveness of CW fNIRS instruments can partially be attributed to the use of off-the-shelf components (16).

The three main components common to all CW fNIRS devices are thoroughly discussed: 1) NIR light emitters, 2) detectors, and 3) means of transporting light to and from the scalp. Typically, a few discrete wavelengths are used in NIRS, and the Modified Beer-Lambert Law (MBLL) equations are evaluated at these selected wavelengths to obtain data on oxygenated and deoxygenated hemoglobin. On the other hand, broadband light sources combined with optical bandpass filters are used in broadband NIRS to obtain continuous absorption spectra of diffuse reflectance. The NIR light needs to be from the NIR part of the spectrum to penetrate the tissue effectively without complete absorption prior to detection, a crucial factor discussed in selecting optimum wavelengths (16).

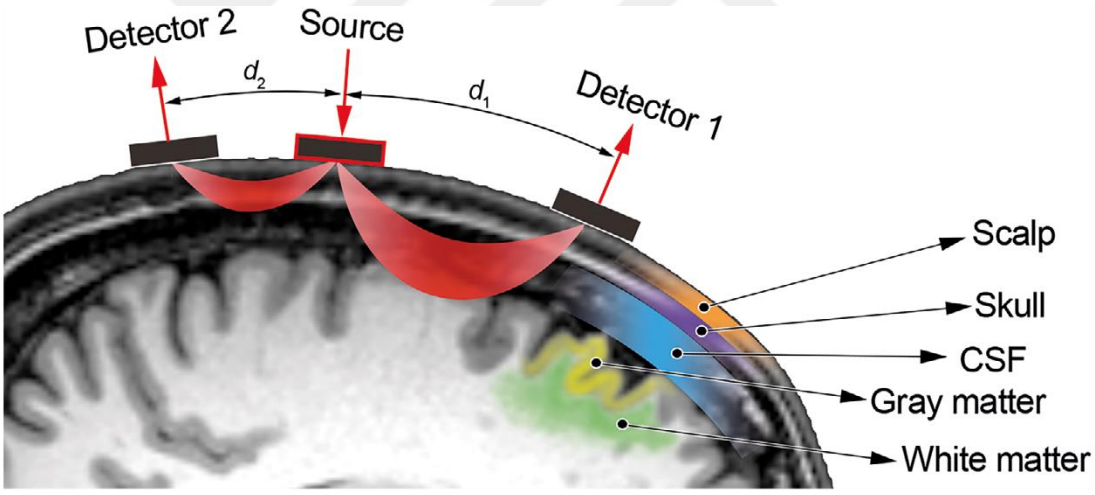

Figure 2.1. The path of Near-Infrared (NIR) photons from the light source to the detector through the head's layers.
Reference: Pinti, P., Tachtsidis, I., Hamilton, A., Hirsch, J., Aichelburg, C., Gilbert, S., & Burgess, P. W. (2020, March). The present and future use of functional near-infrared spectroscopy (fNIRS) for cognitive neuroscience. Annals of the New York Academy of Sciences, 1464(1), 5–29. https://doi.org/10.1111/nyas.13948

Absorption is a process in which the energy of a photon is converted into internal energy in the tissue, and different substances in our body have distinct absorption properties at various wavelengths. Hemoglobin is the dominant absorbing chromophore within the Near-Infrared (NIR) optical window. When a brain area becomes active during a task, the increased metabolic demand leads to an oversupply of regional cerebral blood flow, resulting in changes in hemoglobin concentrations.

Oxygenated hemoglobin (HbO_2) increases, while deoxygenated hemoglobin (HbR) decreases, causing alterations in light attenuation, which can be measured by fNIRS. NIR light also undergoes scattering as it travels through biological tissue, allowing it to penetrate several centimeters. By placing a light detector at a certain distance from the NIR light source, changes in light attenuation can be measured, reflecting variations in HbO_2 and HbR concentrations within the tissue (Figure 2.1) (3).

The Modified Beer Lambert Law (MBLL) is a fundamental principle in Near-Infrared Spectroscopy (NIRS) that relates the attenuation of light to the concentration of absorbing substances in a medium. The law is an extension of the Beer Lambert Law, which describes the relationship between light absorption and concentration in transparent solutions. In NIRS, however, the medium is not fully transparent, and light undergoes both absorption and scattering as it passes through biological tissues.

The MBLL takes into account both absorption and scattering effects, allowing for the quantification of chromophores such as hemoglobin in biological tissues (17). The MBLL equation can be expressed as:

$$\Delta A = log(I_0/I) = \varepsilon * c * d$$

where ΔA is the change in light attenuation (absorbance), I_O is the incident light intensity, *I* is the transmitted light intensity, ε is the molar absorption coefficient of the chromophore, c is the concentration of the chromophore, and d is the pathlength of light through the medium (i.e., the distance between the light source and the detector). The term ΔA is also referred to as the optical density, representing the logarithm of the ratio of incident to transmitted light. It can be also shown as optical density:

$$OD = -log(I/I_0) = \varepsilon CLB + G$$

The optical density (OD) in the Modified Beer Lambert Law (MBLL) is expressed as a logarithmic function of the incident light intensity (Io) divided by the detected light intensity (I). It depends on several factors: the extinction coefficient (ε) of the absorbing substance (chromophore), the concentration (C) of the chromophore in the tissue, the distance (L) between where the light enters and exits the tissue, a pathlength

factor (B) considering the increased photon pathlength due to tissue scattering, and a measurement geometry factor (G) (18).

In NIRS applications, the MBLL is commonly used to estimate changes in the concentrations of oxygenated hemoglobin (HbO2) and deoxygenated hemoglobin (HbR) in brain tissue. When a brain region becomes active, the metabolic demand for oxygen increases, leading to changes in regional cerebral blood flow. This, in turn, alters the concentrations of HbO2 and HbR, resulting in changes in light attenuation, which can be measured by the NIRS device. Despite its simplicity, the MBLL is a powerful tool that allows researchers and clinicians to non-invasively monitor physiological changes in tissues, making it an invaluable technique in various fields, including neuroscience, clinical medicine, and sports science.

Moreover, the MBLL's adaptability to different chromophores and tissues makes it a versatile method for studying and understanding biological processes in living organisms.

Engineers strive to maximize the radiated optical power to enhance signal-to-noise ratio (SNR) and enable the use of longer source-detector distances, which increases sensitivity to deeper tissues. However, tissue heating caused by irradiation or conductive heat transport from the source must be carefully managed to avoid compromising measurements or causing discomfort to subjects. Safety measures are paramount, particularly concerning eye safety for both experimenters and subjects. The emitted light intensity fluctuations can directly affect detector noise, emphasizing the importance of light sources that radiate light as consistently as possible. Proper power circuitry design and stabilization of power supply can mitigate emitter noise.

In fNIRS measurements at several discrete wavelengths, it is desirable to choose light sources with sharply peaked radiation spectra or employ weighted averaging approaches when the emission spectrum is known. Laser diodes (LDs) and light-emitting diodes (LEDs) are the primary light sources utilized in CW fNIRS instruments. LDs offer coherent light emission with narrower bandwidth due to stimulated emission, making them suitable for fiber coupling. However, LDs can be larger and potentially hazardous due to the risks associated with laser radiation for the eyes. On the other hand, LEDs are smaller, come in various emitting wavelengths, and

are considered valid alternatives to LDs, providing flexibility in wavelength selection (16).

The choice between LDs and LEDs depends on specific instrument requirements, including size, weight, power consumption, and fiber coupling efficiency. Each type of light source has its advantages and trade-offs, and their selection is essential in optimizing the performance and capabilities of fNIRS instruments. Overall, CW fNIRS offers engineers a promising and versatile technique for various applications in neuroimaging and other fields, promising insights into brain function and physiological responses (16).

2.3. Noise Problem in fNIRS Signals

Physiological noises originating from various sources, including heartbeat, respiration, Mayer waves, and systemic physiological activity from the outer layers of the brain, as well as motion artifacts, often interfere with event-related functional Near-Infrared Spectroscopy (fNIRS) observations. Consequently, the collected data on cortical activity may be compromised and inaccurate (4).

fNIRS measures the hemoglobin response to brain activation, but it also captures interfering signals from head movement and other physiological changes. These interfering signals can manifest as sudden spikes, baseline shifts, periodic variations, and low-frequency drift in the data. If these confounding factors are not properly addressed, the estimation of the hemoglobin response related to neuronal activity may be biased and inaccurate (19).

A strong cardiac component, which indicates a good optode-scalp coupling, serves as a reliable indicator of high-quality fNIRS signals. This is because the near-infrared light used in fNIRS passes through both the cerebral and superficial layers of the brain. During this journey, various factors, both intrinsic and extrinsic, influence the absorption and scattering of the transmitted light. The intrinsic elements include cerebral and extra-cerebral hemodynamics resulting from systemic artifacts and brain functioning. One such artifact present in both compartments is the heartbeat. Therefore, the presence of the heartbeat in fNIRS data indicates that sufficient light

has reached the brain, and most of the absorption and scattering arise from intrinsic factors. However, if external factors significantly limit the amount of light reaching the brain, leading to poor optode-scalp coupling, the quality of the fNIRS signal may be compromised (20). Extrinsic factors encompass several aspects such as the optode placement tightness, the thickness of the scalp and skull, the properties of the skin, and the density and color of any existing hair. These external elements can influence the quality and reliability of the fNIRS measurements (20). As fNIRS data is collected through the intact skull, extracerebral noises originating from the skin, skull, and blood vessels on the brain's surface are present in every fNIRS channel. Consequently, systemic physiological fluctuations in local hemodynamics are more prone to impact the quality of the fNIRS signal (21).

3. STATE OF THE ART APPROACHES FOR DENOISING AND PREPROCESSING OF FNIRS SIGNALS

In fNIRS data analysis, several methods are employed in a stepwise manner to mitigate noise and artifacts. Various signal processing techniques, including channel exclusion and motion correction, have been devised to address potential confounding factors and eliminate physiological noise from the fNIRS signals. However, selecting the most suitable algorithm or approach can be difficult due to the abundance of different processing methodologies, each offering its own advantages and limitations (22).

3.1. Channel Quality Assessment and Channel Pruning

Various factors can negatively impact the quality of fNIRS signals, including instrument and environmental noise, suboptimal coupling of the optodes to the subject's head, artifacts arising from subject motion, and optical interference caused by the presence of coarse or strongly colored hair. These sources of noise and artifacts can lead to a reduction in the signal-to-noise ratio (SNR) and introduce sudden baseline intensity shifts or sharp spikes in the time series data, thereby jeopardizing the accuracy of the recorded information and subsequent interpretations. To ensure the adequacy of the signal quality, it is imperative to establish a standardized approach for identifying and rejecting subpar channels that could distort the data. One commonly employed criterion involves visually inspecting the optical density signal within the

wavelength range of 830 to 850 nm to ascertain the presence of the heart pulse, either in the time or frequency domain. The rationale behind this approach is grounded in the understanding that fluctuations in optical density are closely associated with physiological hemodynamic changes when a robust and consistent cardiac oscillation is detected. By carefully scrutinizing the fNIRS data in this manner, researchers can effectively discern genuine signals related to brain activity from unwanted noise and artifacts. Rejecting channels with poor signal quality helps enhance the overall robustness and accuracy of the fNIRS measurements, providing a more reliable foundation for subsequent data analysis and scientific interpretations. Moreover, adopting standardized practices for noise reduction and artifact removal is crucial for ensuring the validity and replicability of fNIRS studies across different research settings and experimental conditions (22).

In assessing the quality of fNIRS signals and identifying noise, researchers have two viable options: conducting a simple signal-to-noise ratio (SNR) check or performing spectral analysis to evaluate cardiac power at each channel. The presence and strength of the heartbeat serve as reliable indicators of the optode-scalp coupling and, consequently, serve as effective quality control parameters for fNIRS signals, particularly when the sampling rate is sufficiently high, such as 10 Hz (17).

The visual inspection method for signal quality check has limitations, being subjective, time-consuming, and not ensuring sufficient quality at the 700 nm wavelength (weighted to deoxyhemoglobin, making cardiac pulsation less robust). Automated approaches for channel exclusion are advantageous, especially if they outperform visual assessment. Various automated techniques, including the coefficient of variation (CV) approach, have been suggested to evaluate and determine exclusion pathways (22).

3.2. Motion Artifact Detection

Motion artifacts in fNIRS data are typically identified by detecting rapid signal changes that exceed the amplitude of hemodynamic changes. This detection process involves setting thresholds using user-defined input parameters in motion detection algorithms. By applying these thresholds to different components of the signal, such as moving standard deviation time series, absolute signal amplitude changes, or

standard deviation variations, one can identify temporal epochs likely affected by motion artifacts. However, the use of human input in this process makes it subjective, and optimal parameters may vary across different datasets. An ideal motion artifact detection algorithm should objectively define a threshold based on deviations caused by actual physiological fluctuations, derived directly from the signal itself. By eliminating the reliance on subjective user input and considering actual physiological variations, such an algorithm can enhance the accuracy and reliability of motion artifact identification in fNIRS data (23).

The HOMER2 NIRS processing package includes a motion artifact identification technique called hmrMotionArtifact, which reliably detects motion artifacts based on variations in signal amplitude and/or standard deviation. Motion is identified if the standard deviation increases by a factor greater than SDThresh or if the peak-to-peak amplitude increases by a factor greater than AMPThresh within a window of length tMotion. This technique operates under the assumption that motion artifacts affect multiple channels; hence, signal changes identified as artifacts in one channel are labeled as motion in all channels (24).

3.3. Motion Artifact Correction

3.3.1. Spline Interpolation

Spline interpolation is a commonly used technique in functional near-infrared spectroscopy (fNIRS) data analysis to handle missing or noisy data points. In fNIRS experiments, signal interruptions due to subject motion or other artifacts can lead to gaps in the data, affecting the accuracy of the results. Spline interpolation works by fitting a smooth curve through the existing data points, and then estimating the values for the missing or corrupted data points based on this curve. This method helps to fill in the gaps and produce a continuous, more complete dataset for further analysis. By effectively reconstructing the missing information, spline interpolation enhances the robustness of fNIRS data and facilitates more accurate interpretations of brain activity and hemodynamic responses.

The channel-by-channel method of spline interpolation used suggested by Scholkmann et al. (25). The Homer2 NIRS Processing package utilizes the hmrMotionArtifactByChannel function to automatically identify motion artifact

fragments on a per-channel basis. A cubic spline interpolation is then employed to estimate the motion artifact period. By subtracting the resulting spline interpolation from the original signal, the motion artifact is removed. However, the corrected signal may have different signal levels than the original, necessitating the reconstruction of the time series. While the spline interpolation approach offers the advantage of baseline shift removal, its effectiveness depends on the reliable identification of motion artifacts prior to implementation. If motion artifacts are challenging to detect, the spline method may not yield significant signal improvement (26).

3.3.2. Principal Component Analysis (PCA)

Principal Component Analysis (PCA) is a widely used data analysis technique in functional near-infrared spectroscopy (fNIRS) research. PCA aims to reduce the complexity of fNIRS data by transforming it into a new set of uncorrelated variables called principal components. These components capture the most significant variations in the data and allow researchers to identify patterns and trends more efficiently. By retaining the most informative components and discarding the less relevant ones, PCA helps to reduce noise and highlight the key features of the fNIRS signal related to brain activity. This dimensionality reduction technique enhances data visualization, denoising, and the extraction of meaningful information from large and complex fNIRS datasets, making it a valuable tool in neuroimaging studies.

PCA implementation in fNIRS involves converting an N-measurement dataset into N linearly uncorrelated components, sorted based on their contribution to the data variance. In many cases, motion artifacts are more prominent than the actual NIRS background signal, and they may affect multiple NIRS channels. To address this, PCA is applied with the assumption that the first R principal components primarily represent motion artifacts, capturing the majority of the variance. By removing these R components from the data, researchers can filter out the motion artifacts and proceed with further analysis of the NIRS data, focusing on the relevant brain-related signal. This approach helps enhance the accuracy and reliability of fNIRS data interpretation by mitigating the influence of motion artifacts (24). The number of measurements available (N) and the number of components removed (R) have a direct impact on PCA performance (26).

If PCA is applied to data points presumed to contain motion artifacts, it is less probable that the physiological fluctuations in the motion-free part of the signal will be effectively removed. Therefore, accurate identification of motion artifacts is crucial when using PCA to address such issues in the data (23).

3.3.3. Independent Component Analysis (ICA)

Independent Component Analysis (ICA) is a powerful data analysis method frequently employed in functional near-infrared spectroscopy (fNIRS) research. Unlike PCA, which transforms data into uncorrelated components, ICA aims to extract statistically independent components from the fNIRS signal. These components represent different physiological or neural processes contributing to the data. By separating the underlying sources of signal variation, ICA allows researchers to identify distinct brain-related activities, such as hemodynamic responses to specific stimuli or cognitive tasks, even in the presence of artifacts or overlapping signals. ICA has proven valuable for denoising fNIRS data, enhancing brain signal localization, and uncovering relevant brain networks. Its ability to separate mixed signals into meaningful sources makes ICA a valuable tool for advancing our understanding of brain function and connectivity in fNIRS neuroimaging studies.

Numerous research groups have explored the utility of independent component analysis (ICA) in differentiating functional optical responses (FORs) from noise in raw NIRS time series. The findings suggest that ICA holds promise as an effective method for detecting fast neuronal signals. By using ICA, researchers can successfully eliminate non-relevant noises, allowing them to focus on identifying the specific FORs present in the NIRS data.

Subsequently, event-related averaging is utilized to pinpoint and analyze the Fast Optical Responses (FORs) across the NIRS time series. Overall, ICA offers a valuable approach for improving the accuracy and sensitivity of detecting important brain activity patterns in fNIRS studies (27).

3.3.4. Wavelet Analysis

A Wavelet analysis is a valuable signal processing technique widely employed in functional near-infrared spectroscopy (fNIRS) research. This method allows

researchers to investigate the time-frequency characteristics of the NIRS signal, providing insights into the dynamic changes in brain activity. By applying wavelet transforms to the fNIRS time series, researchers can identify localized changes in brain hemodynamics at different time scales. This capability is especially useful for studying transient brain responses, such as task-related activations or event-related hemodynamic fluctuations. Wavelet analysis enhances the temporal resolution of fNIRS data, enabling the detection of fast and brief neural responses. Its versatility and ability to capture both frequency and temporal information make wavelet analysis a valuable tool for investigating complex brain processes in fNIRS neuroimaging studies.

In wavelet analysis, each channel's data series undergoes discrete wavelet transform with multiple levels of decomposition, determined by the time series duration. This process yields detail and approximation coefficients for each level. The hemodynamic response, being smoother and slower than motion artifacts, creates a linear combination with the artifacts in the measured signal. The detail wavelet coefficients exhibit a Gaussian probability distribution. By assuming that coefficients related to evoked responses will center around zero with minimal variation, it becomes possible to identify outliers as coefficients representing motion artifacts. These outliers can be set to zero to eliminate motion distortions in the temporal time-series before reconstructing the signal using inverse discrete wavelet transform. This approach aids in separating the physiological signal of interest from unwanted artifacts in fNIRS data (26).

3.4. Bandpass Filtering

Bandpass filtering is frequently used to eliminate very low (0.01 Hz) and very high (0.2 Hz; heartbeat, respiration rate, instrument noise) frequency information from the stream. For noise reduction, a variety of filters have been used in fNIRS research, with the Butterworth filter being the most often used. Other filters utilized include zero-phase Fast Fourier Transform (FFT) filters, elliptic filters, moving average filters and Chebyshev filters (22).

The Butterworth filter is a commonly used type of bandpass filter in fNIRS data processing. It is characterized by a flat frequency response in the passband and a steep

roll-off in the stopband. This filter is effective in removing noise and artifacts from the fNIRS signal while preserving the frequency content of interest. The order of the Butterworth filter can be adjusted to control the sharpness of the roll-off, allowing researchers to tailor the filter to their specific data requirements (28).

The Chebyshev filter is another type of bandpass filter that is often used in fNIRS data analysis. It provides a steeper roll-off in the stopband compared to the Butterworth filter but may introduce ripples in the passband. This filter is useful when a more aggressive noise reduction is needed, but it may come at the cost of slight distortion in the frequency response. Like the Butterworth filter, the Chebyshev filter's order can be adjusted to achieve the desired level of noise attenuation (22).

The moving average filter is a simple and intuitive type of bandpass filter used in fNIRS signal processing. It works by averaging adjacent data points within a specified window, effectively smoothing the signal and removing high-frequency noise. This filter is particularly useful for reducing motion artifacts and other high-frequency noise sources. However, it may also blur the fine temporal details of the signal, and the window size needs to be carefully chosen to strike a balance between noise reduction and signal preservation (28).

The zero-phase Fast Fourier Transform (FFT) is a powerful technique used for frequency-domain signal processing. It is commonly employed to investigate the frequency content of fNIRS signals and identify specific frequency components related to neuronal activity or physiological changes. The zero-phase FFT ensures that the phase information of the signal is preserved during the transformation, allowing for accurate time-domain reconstruction after frequency analysis. By examining the power spectral density obtained through the FFT, researchers can identify dominant frequency peaks that correspond to hemodynamic responses or other relevant physiological phenomena. This technique enables a deeper understanding of the underlying neurovascular dynamics and provides valuable insights into brain activation patterns and responses to different stimuli. Additionally, the zero-phase nature of the FFT minimizes potential phase distortions that could arise from typical FFT implementations, making it a reliable and widely used tool in fNIRS research (22).

3.5. Correlation-based Signal Improvement (CBSI)

Correlation-based signal improvement in fNIRS is a data preprocessing technique aimed at enhancing the quality of the recorded signals by reducing noise and extracting meaningful hemodynamic responses. This method relies on the assumption that genuine functional responses to brain activity are correlated across different channels, while noise and artifacts tend to be uncorrelated or less correlated. The process involves computing the cross-correlation matrix among all the channels in the dataset and identifying the dominant correlated components. The correlated components are then combined linearly to generate a weighted sum, effectively enhancing the signal-to-noise ratio and highlighting the genuine physiological responses (23).

One of the advantages of correlation-based signal improvement is its ability to address common noise sources affecting multiple channels simultaneously. This includes systemic physiological noises, motion artifacts, and environmental interference. By leveraging the collective information from all channels, the technique is robust in handling noise that affects the entire data set.

Moreover, it is non-parametric and does not assume any specific noise distribution, making it flexible and applicable in various experimental scenarios (27).

However, the correlation-based signal improvement method also has its limitations. For instance, it requires a sufficient number of channels and assumes that the genuine signals are correlated across them, which may not always hold true in certain experimental setups. Additionally, the technique may not be effective in cases where the noise is highly correlated across channels, leading to limited improvements in the signal quality (27).

Overall, correlation-based signal improvement is a valuable tool in fNIRS data preprocessing, offering an effective means to enhance signal quality, identify relevant brain activation patterns, and improve the accuracy of functional neuroimaging studies. Researchers often combine this technique with other preprocessing methods to optimize data quality and ensure reliable interpretations of fNIRS results.

3.6. Short Separation Regression

Short separation detectors, a recent breakthrough in the field, have emerged as a revolutionary technique in fNIRS. These detectors are strategically positioned in the activation region with a source-detector distance of less than one centimeter, making them highly sensitive to the superficial layers of the brain. In this method, the signal from long separation detectors captures both brain and surface layer activities, while the signal from short separation detectors predominantly represents superficial brain layers. By applying regression to subtract the short separation signal from the long separation signal, the unwanted superficial component is effectively filtered out, leaving behind a more accurate representation of brain activity. This innovative approach enhances the precision of fNIRS measurements and opens new possibilities for deeper insights into brain function and activation patterns (29).

3.7. General Linear Model (GLM) Analysis

General Linear Model (GLM) refers to a statistical method used to model and analyze the hemodynamic response of the brain to specific experimental conditions or tasks. In fNIRS studies, researchers often design experiments to investigate brain activity associated with certain cognitive tasks, stimuli, or conditions. The GLM analysis allows us to examine how changes in the concentration of oxyhemoglobin (HbO2) and deoxyhemoglobin (HbR) are related to these experimental factors. The GLM analysis involves creating a mathematical model that describes the relationship between the measured fNIRS data and the experimental design. It includes regressors or predictors representing the different experimental conditions or events, and the goal is to estimate the contribution of each predictor to the observed changes in hemoglobin concentrations. GLM is a popular choice for analyzing group-level differences or conditions due to its straightforward application with multi-level analysis and its ability to average away between-subject variance, revealing substantial group variations. However, at the individual subject level, the accuracy of modeling brain activation using general linear regression is limited by the significant variability in the shape and timing of each person's hemodynamic response (22).

The GLM analysis is widely used in fNIRS research because it provides a flexible and powerful framework for hypothesis testing and inference. It allows researchers to determine whether there are significant differences in brain activity across different experimental conditions and provides insights into the underlying neural processes associated with cognitive tasks or stimuli.

4. MATERIALS AND METHODS

An Ethics Committee approval has been obtained with reference number 52020640814625 at Macquarie University, and fNIRS data collected during an auditory task will be used for analysis. The data is publicly available and presented at the following link:

"**https://openfnirs.org /community/ fresh/welcome-to-the-fnirs-fresh-project/**".

4.1. Experimental Protocol

4.1.1. Participants

A total of seventeen individuals willingly participated in this research project. Each participant confirmed that they had no prior history of hearing issues. The age range of the participants spanned from 22 to 40 years, indicating a diverse age group within the study cohort (30).

During the experiment, participants were seated in a sound-attenuating booth, providing a controlled and quiet environment. To ensure their comfort throughout the study, they were provided with comfortable chairs. The entire experiment lasted approximately 25 minutes, during which the participants were asked not to focus on the sounds being presented. To make the experimental setting more pleasant, participants were given the option to watch a subtitled film without sound. Out of the seventeen participants, seven individuals chose to accept this option, while the rest opted to solely participate in the auditory task without any visual distraction (30).

4.1.2 Materials

The NIRS data were collected using a NIRx NIRScoutX device equipped with APD (Avalanche Photodiode) detectors. The recorded data were stored on a disk at a sampling rate of 5.2 Hz. For the fNIRS optode-cap configuration, a total of 12 source channels and 12 detector channels were utilized. Additionally, eight short detectors were strategically placed across the participant's head to enhance the coverage and sensitivity of the measurements. This setup allowed for comprehensive monitoring and analysis of the hemodynamic responses during the experiment (30).

4.1.3 Experimental Design

During the experiment, participants experienced 3 different stimulus conditions. These are

1)Speech
2)Noise
3)Silence

The speech stimulus was created by concatenating three sentences from the AusTIN speech corpus, with a combined duration of 5.25 seconds. For the noise stimulus, a range of frequencies between 300 and 700 Hz was uniformly distributed, resulting in a 5-second duration noise clip. The control condition involved 5 seconds of complete silence. To ensure variability and prevent predictability, the stimuli were presented in a random order for each participant. Additionally, the inter-stimulus interval, which denotes the time between the end of one stimulus and the beginning of the next, was randomly chosen for each trial from a uniform distribution spanning 10 to 20 seconds. In total, there were 20 trials for each stimulus condition, resulting in a comprehensive set of 60 trials per participant. This design allowed researchers to obtain robust and diverse data across the different stimulus conditions, ensuring a thorough investigation of the brain's response to speech, noise, and silence (30).

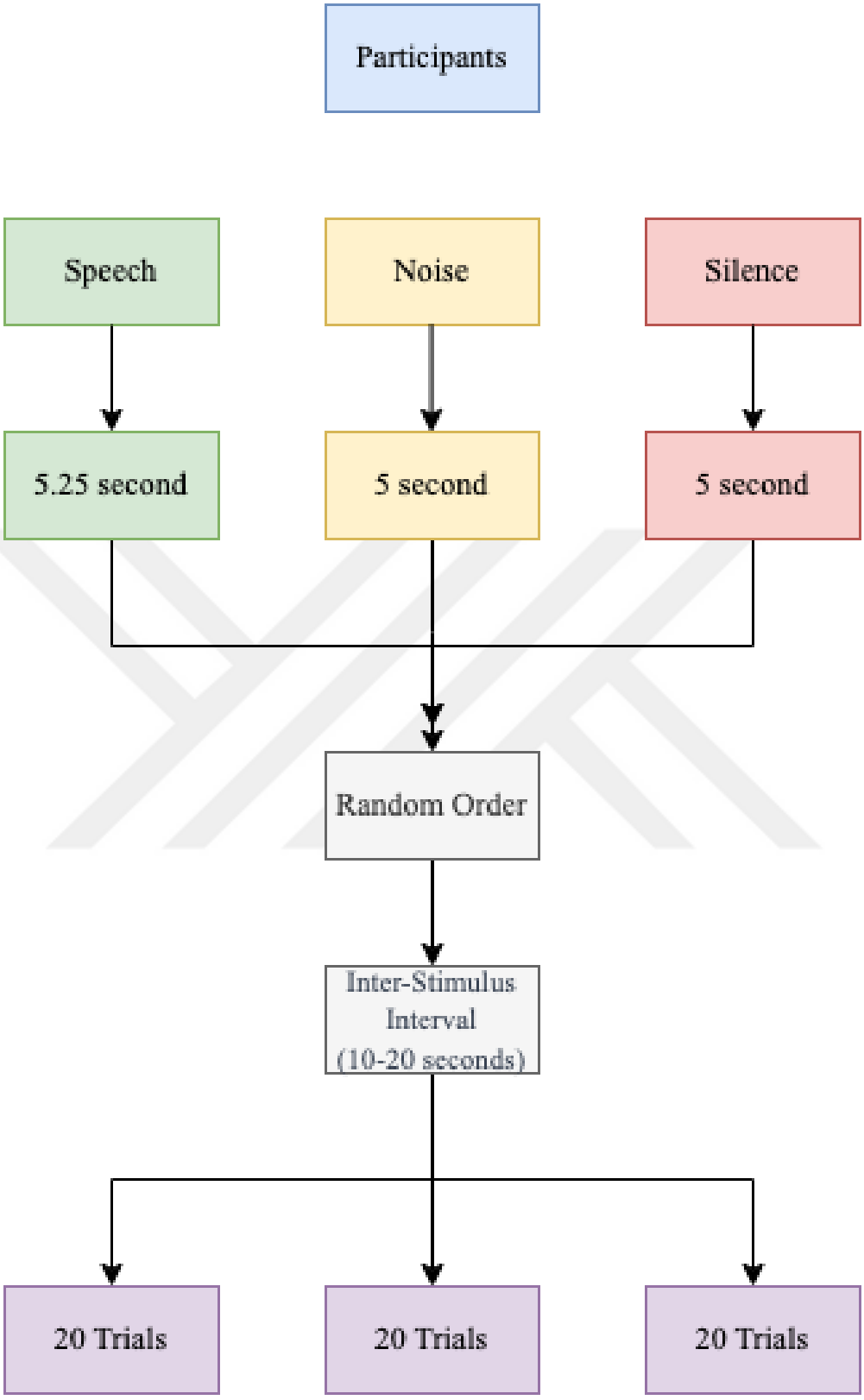

Figure 4.1. Experimental Procedure

4.2. FNIRS Data Analysis

4.2.1. Processing Pipeline Steps

In this study, 4 main fNIRS processing pipelines were implemented. A comparison has been made about which of these pipelines is better. These pipelines can include motion correction with Spline SG, short channel regression, bandpass filter and correlation based signal improvement. They are employing various functions from the Homer library.

4.2.1.1 Processing Pipeline 1

The first processing pipeline starts by loading the subject data from the specified directory. The data consists of near-infrared spectroscopy (NIRS) recordings collected during a cognitive task.

The pipeline first separates the two wavelengths (760nm and 850nm) of the NIRS signal and converts the raw intensity data to optical density (dod) data. Motion artifacts are detected using the "hmrR_MotionArtifactByChannel" function of Homer3 and pruned using the "hmrR_PruneChannels" function of Homer3. It then proceeds to convert the dod data into hemoglobin concentration changes (HbO and HbR) using the "hmrR_OD2Conc"function of Homer3. No motion correction is applied at this stage.

The pipeline then applies a bandpass filter by using "hmrR_BandpassFilt" function of Homer3 to the HbO and HbR signals to remove unwanted frequency components, such as physiological noise and motion artifacts. Following this, short-channel regression is employed, which involves finding the short-channel with the maximum correlation to each channel and regressing out its influence on the respective channel's HbO and HbR signals.

Next, the pipeline takes block averages of the bandpass filtered HbO and HbR signals for each condition in the cognitive task to improve the signal-to-noise ratio. Subsequently, the pipeline performs correlation-based signal improvement to refine the motion-corrected HbO and HbR signals. It calculates the correlation between each long channel's signal and the short channels' signals and then regresses out the contribution of the short channel with the highest correlation. The resulting HbO and HbR signals are now less affected by motion artifacts.

Throughout the pipeline, quality control measures are applied, such as determining signal-to-noise ratios and masking out channels with low SNR. Moreover, the pipeline utilizes event-related regressors to align the data with the timing of the cognitive task events, allowing for precise data selection for each condition.

After processing all the subjects' data through the pipeline, the results are saved as block-averaged data for further analysis. The processed data is now ready for statistical comparisons, hypothesis testing, or any other analyses related to the cognitive task or experimental design.

4.2.1.2 Processing Pipeline 2

The processing pipeline 2 involves a series of steps to analyze audio fNIRS data. First, the raw data is loaded for each subject and session, and the short channel data is extracted from the two wavelengths (760 nm and 850 nm) of each channel.

Motion artifacts are detected using the “hmrR_MotionArtifactByChannel” function of Homer3 and pruned using the “hmrR_PruneChannels” function of Homer3. The motion correction step is performed using the Spline SG method with “hmrR_MotionCorrectSplineSG” function of Homer3 , which helps to correct for motion-induced artifacts in the optical density data. The corrected optical density data is converted to hemoglobin concentration data (HbO and HbR) through conversion algorithms. Bandpass filtering is applied to these data by using “hmrR_BandpassFilt”function of Homer3 to further clean the signals in the frequency range of interest.

Next, short channel regression is performed to eliminate the impact of short channels on the target channel's hemoglobin signal. This step helps to mitigate the influence of superficial layers in the brain.

A block averaging technique is employed to enhance signal-to-noise ratio by averaging the hemoglobin signals within each block of trials. Correlation-based signal improvement (CBSI) is then implemented to refine the hemoglobin signals. The method calculates an optimal weighting factor that balances the contribution of HbO and HbR signals to improve the overall signal quality.

Another block averaging step is performed after CBSI to enhance the data quality further. Finally, the processed data is saved for further analysis. The pipeline is executed for multiple subjects and sessions, and the results are stored in separate data files.

The difference between these two pipelines is that the first pipeline did not contain motion correction, while the second pipeline contained motion correction with spline SG. So that we can compare the difference of including motion correction and not including motion correction.

4.2.1.3 Processing Pipeline 3

The third processing pipeline the begins by loading the raw fNIRS data for each subject and session. After loading, the script proceeds with necessary preprocessing steps, including the extraction of the raw intensity data for both wavelengths (760 nm and 850 nm) from each channel. Additionally, the pipeline identifies and removes motion artifacts by calculating the motion artifact index for each channel using the "hmrR_MotionArtifactByChannel" function from Homer3 and pruned using the "hmrR_PruneChannels" function of Homer3.

To distinguish short channels from long channels, a predefined set of short channels is determined based on their anatomical location. The pipeline identifies the short channel indices and separates them from the rest of the channels (long channels) for further analysis.

The raw intensity data is converted to optical density (OD) data using the "hmrR_Intensity2OD" function from Homer3. OD data is preferred for fNIRS analysis as it minimizes the effects of variations in light source intensities and provides a more stable baseline.

After obtaining OD data, the pipeline proceeds to calculate the changes in hemoglobin concentrations (HbO and HbR) using the "hmrR_OD2Conc" function from Homer3. The conversion is performed based on the modified Beer-Lambert law, considering the differential pathlength factor (DPF) and molar extinction coefficients for HbO and HbR at 760 nm and 850 nm wavelengths. Next, the pipeline applies bandpass filtering to the hemoglobin concentration data using the

“hmrR_BandpassFilt" function from Homer3. This step removes unwanted frequencies and noise outside the frequency range of interest (typically 0.01 Hz to 0.5 Hz for fNIRS).

To further enhance the signal quality, the pipeline utilizes correlation-based signal improvement (CBSI) with the “hmrR_MotionCorrectCbsi" function from Homer3. CBSI corrects for motion artifacts by estimating motion artifacts using the data from nearby short channels and then removes them from the target channel.

The pipeline performs Short Separation Regression (SSR) to minimize the influence of short channels on long channels. This step uses the hemoglobin concentration data from short channels to predict and remove the unwanted signals from long channels, effectively reducing contamination from superficial layers.

To improve the signal-to-noise ratio and obtain a more robust response estimate, the pipeline applies block averaging to the processed hemoglobin concentration data. The epochs corresponding to different auditory stimuli are averaged to obtain more reliable and smoother hemodynamic responses.

The pipeline is applied to multiple subjects and sessions, and the processed data is stored separately for each subject. The functions utilized from Homer3 include “hmrR_MotionArtifactByChannel”,“hmrR_PruneChannels”, “hmrR_Intensity2OD”, “hmrR_OD2Conc”, “hmrR_BandpassFilt”, and “hmrR_MotionCorrectCbsi”.

The most crucial difference from first two pipeline is the third pipeline implements firstly CBSI and then Short Separation Regression (SSR). In this way, we can compare the effects of applying SSR and CBSI in different order.

4.2.1.4 Processing Pipeline 4

The pipeline starts with data loading and preprocessing for each subject and session. The fNIRS data is loaded from SNIRF files, and the raw intensity data for both wavelengths (760 nm and 850 nm) is extracted for each channel. Motion artifacts are detected and marked using the "hmrR_MotionArtifactByChannel" function from Homer3 and pruned using the “hmrR_PruneChannels” function of Homer3. Additionally, short channels are identified based on their anatomical location, and the long channels are separated from them.

The raw intensity data is converted to optical density (OD) data using the "hmrR_Intensity2OD" function from Homer3. OD data minimizes the impact of light intensity variations and provides a stable baseline for further analysis.

Motion-corrected optical density data is obtained using the Spline SG method for motion correction, implemented in the "hmrR_MotionCorrectSplineSG" function from Homer3. This method efficiently removes motion artifacts while preserving the underlying neurovascular signals.

The motion-corrected optical density data is converted to changes in hemoglobin concentrations (HbO and HbR) using the "hmrR_OD2Conc" function from Homer.3 This step involves applying the modified Beer-Lambert law with appropriate parameters, including the differential pathlength factor (DPF) and molar extinction coefficients.

Next, the pipeline applies bandpass filtering to the hemoglobin concentration data using the "hmrR_BandpassFilt" function from Homer. Bandpass filtering removes unwanted frequencies outside the range of interest (typically 0.01 Hz to 0.5 Hz) to enhance the signal-to-noise ratio.

The pipeline applies correlation-based signal improvement (CBSI) to further enhance the signal quality and reduce residual motion artifacts. The "hmrR_MotionCorrectCbsi" function from Homer3 is utilized for this purpose.

To minimize the influence of short channels on long channels, the pipeline performs Short Separation Regression (SSR). For each long channel, the short channel with the highest correlation is identified, and the impact of this short channel on the long channel's hemoglobin concentration data is linearly regressed out.

The processed hemoglobin concentration data is then block-averaged to improve the signal reliability. The data is divided into epochs corresponding to different auditory stimuli, and each epoch is averaged to obtain more robust and smoother hemodynamic responses.

The pipeline is applied to multiple subjects and sessions, and the processed data is stored separately for each subject. Throughout the pipeline, several functions from Homer 3 are utilized, including “hmrR_MotionArtifactByChannel", “hmrR_PruneChannels", “hmrR_Intensity2OD", “hmrR_MotionCorrectSplineSG", “hmrR_OD2Conc", “hmrR_BandpassFilt", and “hmrR_MotionCorrectCbsi”.

This processing pipeline 4 including motion correction with spline SG, different to the processing pipeline 3. So that we can see the effect of applying motion correction with spline SG.

After this step, we separated these 4 main pipelines into 10 methods to see effects of each steps. We started to analyze each method separately.

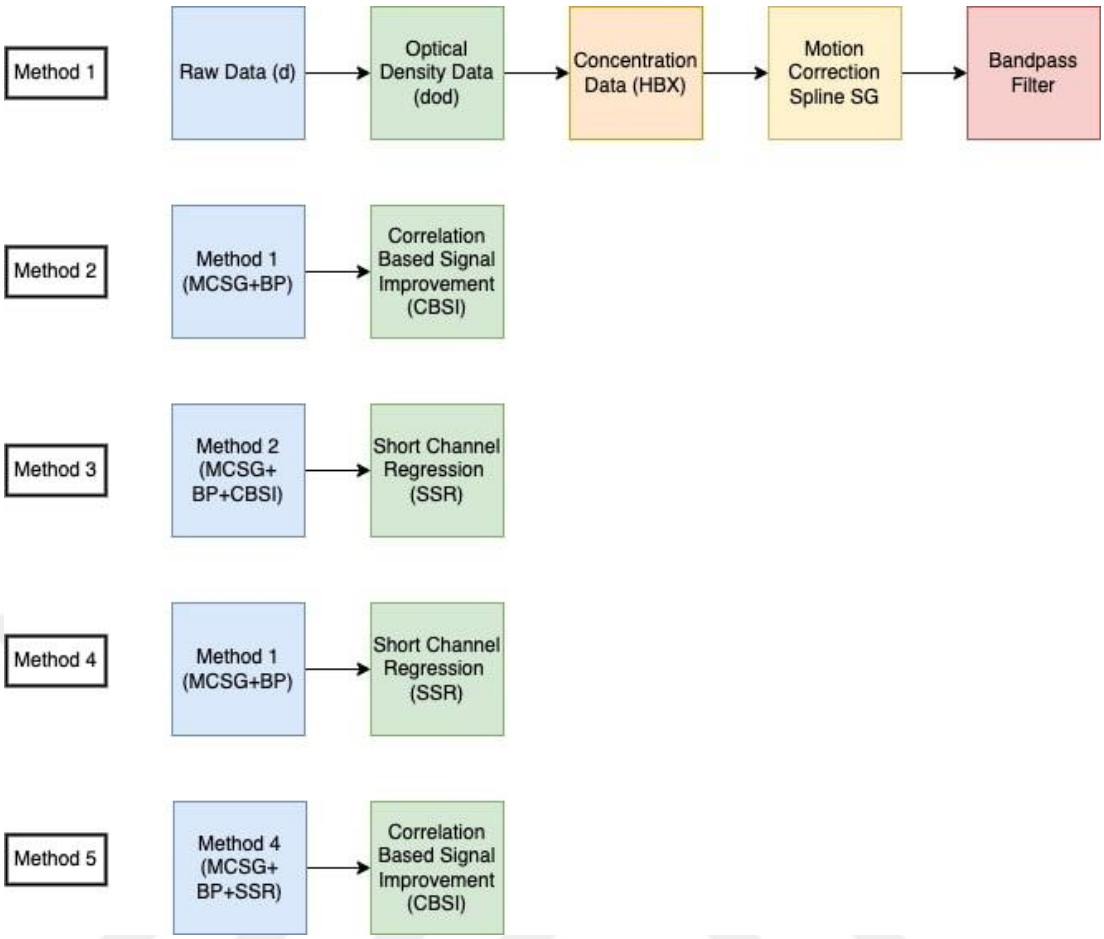

Figure 4.2. Methods 1, 2, 3, 4, and 5 are derived from 4 main pipelines for comparative analysis.

Figure 4.2. shows the first 5 methods which are derived from 4 main pipelines that we created. These 5 methods mainly focuses on Motion Correction with Spline SG and other filtering techniques (Bandpass filter, Correlation Based Signal Improvement (CBSI), and Short Separation Regression (SSR)).

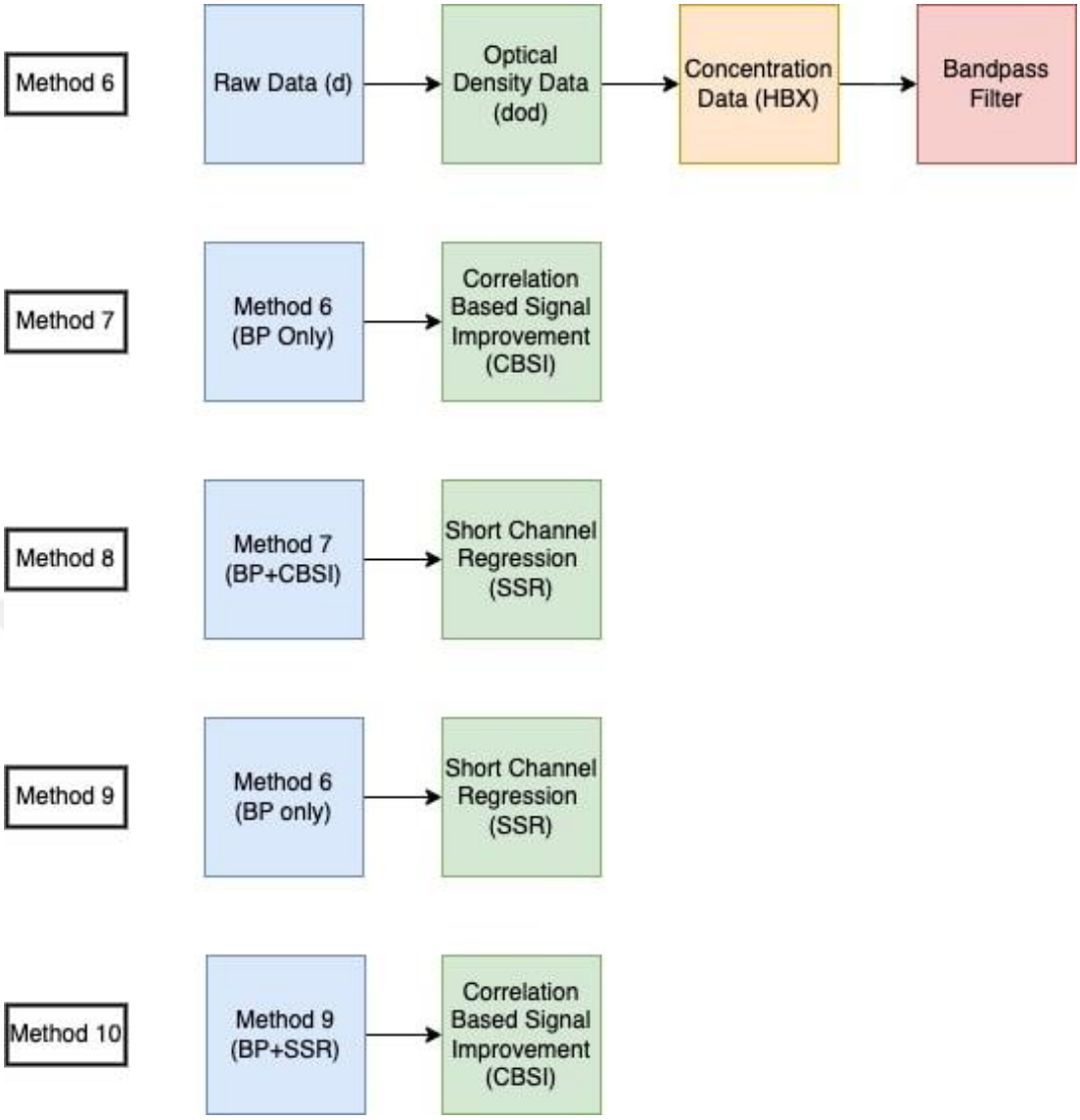

Figure 4.3. Methods 6, 7, 8, 9, and 10 are derived from 4 main pipelines for comparative analysis.

Figure 4.3. shows the other 5 methods which are derived from 4 main pipelines that we created. These 5 methods do not include Motion Correction with Spline SG. However, they mainly include other filtering techniques (Bandpass filter, Correlation Based Signal Improvement (CBSI), and Short Separation Regression (SSR)).

Then we calculated Time to Peak (TTP) values for all methods, factoring in 17 subjects, 25 channels, and 3 stimuli. This involves extracting relevant data, determining peak indices within a specified time window, and subsequently computing TTP by combining peak indices with the window's starting point. The resulting TTP values are summarized, offering insights into method-specific performance. For each method, mean and standard deviation of TTP values are computed across stimuli and subsequently normalized with the sampling rate. The final outcome consists of matrices (P1 to P10), encapsulating summarized TTP values for each method and stimulus.

TTP refers to the moment at which a hemodynamic signal, typically representing changes in oxygenated and deoxygenated blood concentrations, reaches its peak amplitude in response to a neural stimulus or cognitive task. This temporal landmark is of paramount importance as it provides insights into the underlying neurovascular coupling processes that link neural activity with changes in blood flow and oxygenation levels. TTP reflects the intricate interplay between neural activation, metabolic demand, and subsequent hemodynamic adjustments in the brain. It offers a window into the temporal aspects of neural processing, shedding light on how different brain regions and channels respond to stimuli over time.

Then we implemented Contrast to Noise Ratio (CNR). This section employs nested loops and calculates the CNR for each combination of methods, subjects, channels, and stimuli. The CNR is calculated based on the mean of an active data window divided by the square root of the sum of the standard deviations of the active and baseline data windows.

Contrast-to-Noise Ratio (CNR) is a quantitative measure used in functional Near-Infrared Spectroscopy (fNIRS) studies to assess the quality of the recorded hemodynamic signals, specifically the contrast between the signal of interest and the noise present in the data. A higher CNR value indicates a stronger and more detectable hemodynamic response relative to the background noise, which is crucial for accurate and meaningful interpretation of the data.

We can use CNR as a tool to determine the effectiveness of experimental designs, assess the sensitivity of the fNIRS system, and optimize data acquisition parameters such as the number of trials, stimulus intensity, and duration.

Following the CNR computation, we proceed to conduct one-sample t-tests on the CNR data, aiming to assess the statistical significance of differences between methods and stimuli. Through the t-test we calculated key statistical measures including the test statistic, p-value, and confidence interval. These outcomes serve as crucial indicators of whether the observed differences in CNR values are statistically significant. Then we compile the results of the t-tests into a multidimensional matrix termed 'Thr_Tsats'. Each element of this matrix reflects the t-test outcome, wherein the presence or absence of statistical significance is denoted by a binary variable 'h'. The t-statistic is further incorporated into this matrix, potentially offering insights into the direction and magnitude of differences between groups. The 'Thr_Tsats' matrix enables comprehensive visualization of the t-test results, as it generates a set of subplots with heatmaps. These heatmaps provide an intuitive representation of the t-test outcomes for different methods and channels per stimulus, facilitating the identification of patterns and relationships within the data.

A one-sample t-test is a statistical hypothesis test that is used to determine whether the mean of a single sample of data significantly differs from a specified population mean or a hypothesized value. It assesses whether the sample's mean is statistically different from the expected value, and it provides a measure of how likely any observed differences are due to random chance. In the context of functional Near-Infrared Spectroscopy (fNIRS), a one-sample t-test can be applied to investigate whether the mean of a certain hemodynamic response, such as changes in oxygenated or deoxygenated hemoglobin concentration, significantly differs from a reference value.

5. RESULTS AND DISCUSSION

Time to Peak

	Stim 1	Stim 2	Stim 3
M1 (MCSG+BP)	8.78 ± 2.53	9.47 ± 2.62	9.52 ± 3.04
M2 (MCSG+BP+CBSI)	9.32 ± 2.68	9.97 ± 2.57	9.93 ± 3.01
M3 (MCSG+BP+CBSI+SS)	10.32 ± 3.08	10.01 ± 2.82	10.40 ± 3.00
M4 (MCSG+BP+SS)	10.08 ± 3.30	9.65 ± 2.87	10.08 ± 3.10
M5 (MCSG+BP+SS+CBSI)	10.09 ± 3.06	9.86 ± 2.69	10.32 ± 3.04
M6 (BP ONLY)	9.09 ± 2.24	9.53 ± 2.40	9.83 ± 2.91
M7 (BP+CBSI)	9.60 ± 2.33	10.06 ± 2.31	9.91 ± 2.82
M8 (BP+CBSI+SS)	10.63 ± 2.68	10.09 ± 2.39	10.35 ± 2.78
M9 (BP+SS)	10.18 ± 2.99	9.61 ± 2.51	10.04 ± 2.77
M10 (BP+SS+CBSI)	10.30 ± 2.69	10.10 ± 2.37	10.16 ± 2.77

Table 5.1. Time to Peak (TTP) values for 10 methods and 3 stimulus type (speech, noise, silence)

Table 5.1. demonstrates the results of Time to Peak values for 10 methods and 3 stimuli. We calculate them to determine the ideal activation interval for these methods. We took the mean of the TTP values over all methods, channels and stimuli types and computed the grand average value as 10.45 $\pm$ 3.03 seconds as a result. We used 3 seconds as a prestimulus baseline and determined the activation interval between 4 and 10 seconds after onset of stimulus for each truncated block signal.

Channel Numbers

Channel Number Before Short Channel Removal	Channel Number After Short Channel Removal	Channel Number Before Short Channel Removal	Channel Number After Short Channel Removal
1	1	19	14
3	2	20	15
4	3	21	16
6	4	22	17
7	5	23	18
8	6	24	19
9	7	26	20
11	8	27	21
12	9	28	22
13	10	29	23
14	11	31	24
16	12	32	25
17	13		

Table 5.2. Channel Numbers before and after short channel removal

Table 5.2. demonstrates the numbers assigned to each long channel before and after short channel removal. In the beginning, there were 33 channel recordings in each experimental session which consisted of 25 long and 8 short channels. However, we removed the 8 short channels and utilized 25 channel data for further analysis. Those short channels were 2, 5, 10, 15, 18, 25, 30, and 33.

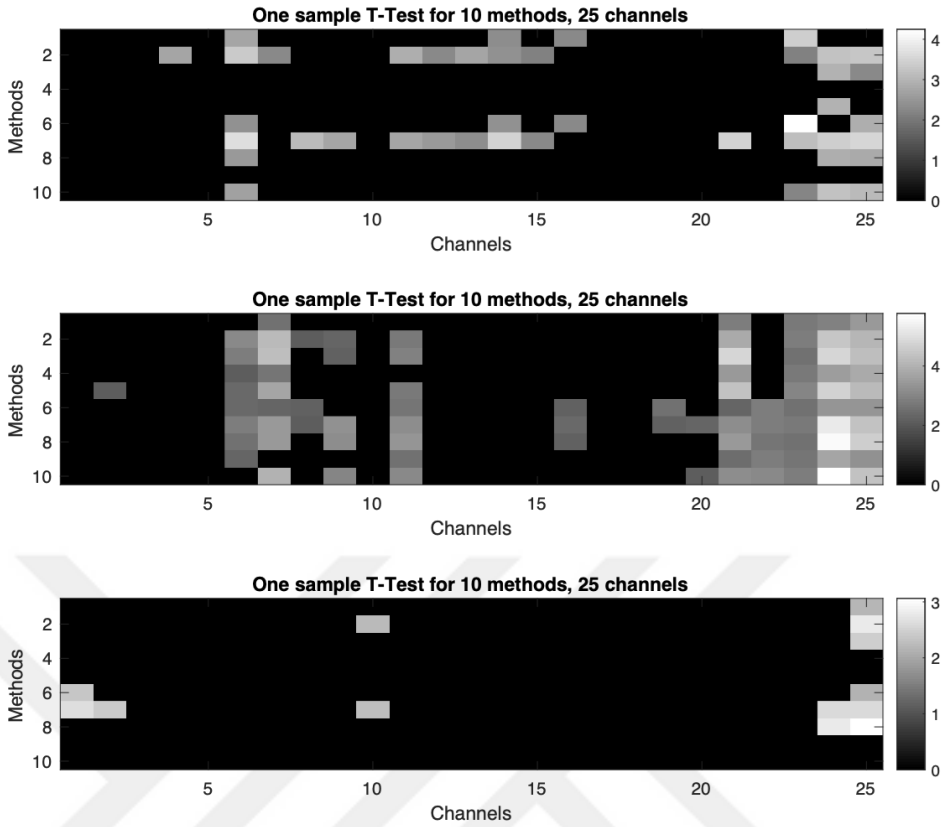

Figure 5.1. Heat map of one sample T-Test for 3 stimulus, 10 methods, 25 channels

Figure 5.1. shows the heat map of one sample t-test results for 3 stimuli types (speech, noise, silence), 10 methods, 25 channels. The x-axis represents the channels, and the y-axis represents the methods. By looking at the intersection of a channel and method, we can gauge the significance level of the t-test for that specific combination. In this figure, black colored pixels correspond to non-significant results (i.e. channels with t values that could not surpass the $p<0.05$ threshold) and light colored pixels correspond to channel data that resulted in statistically significant activation where lighter colors denote higher significant activation. Shades of gray between black and white represent varying levels of statistical significance. Darker areas suggest that the null hypothesis is not rejected, indicating no significant difference in CNR values for that method-channel pair. Lighter areas indicate significant differences in CNR values, implying that the null hypothesis is rejected, and there's a likely genuine difference. By comparing the heat maps for different stimuli, we can observe if the significance patterns remain consistent or differ across the 3 auditory stimuli.

This might reveal whether the effects being measured are stimulus-specific or consistent across different conditions.

By examining the heat map in detail, we determined which channels had significant activation for both speech and noise stimuli. Channel 6 and channel 25 had significant activation for both stimuli. They were the most active channels. Therefore, these 2 channels were selected to analyze. Channel 6 represents left Heschl's Gyrus and channel 25 represents right Heschl's Gyrus in the brain. Our regions of interest (ROI) are left Heschl's Gyrus and right Heschl's Gyrus.

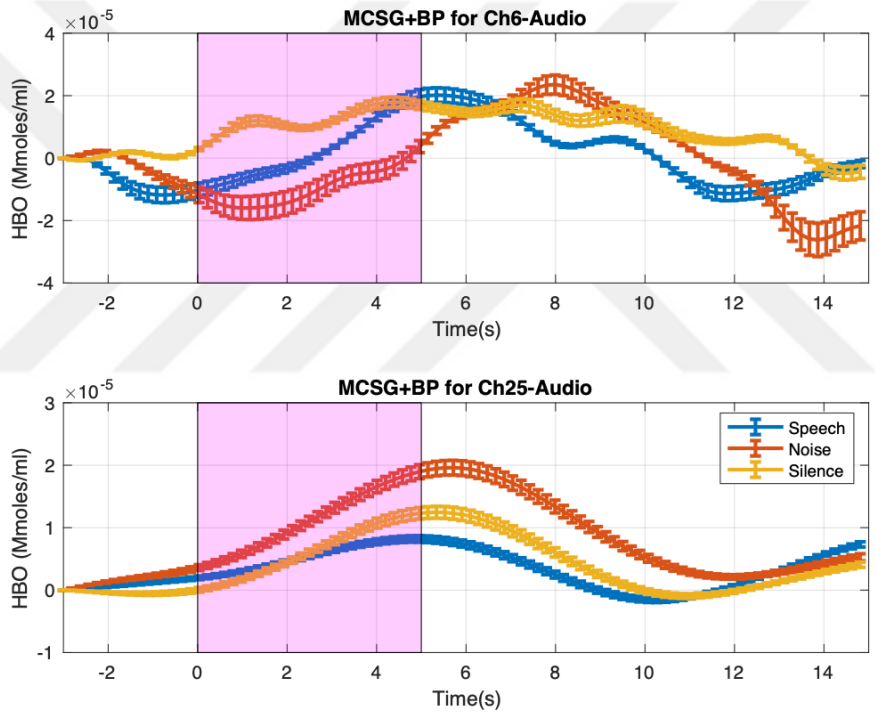

Figure 5.2. Block Average result of Method 1 (MCSG + BP) for Channel 6 and Channel 25

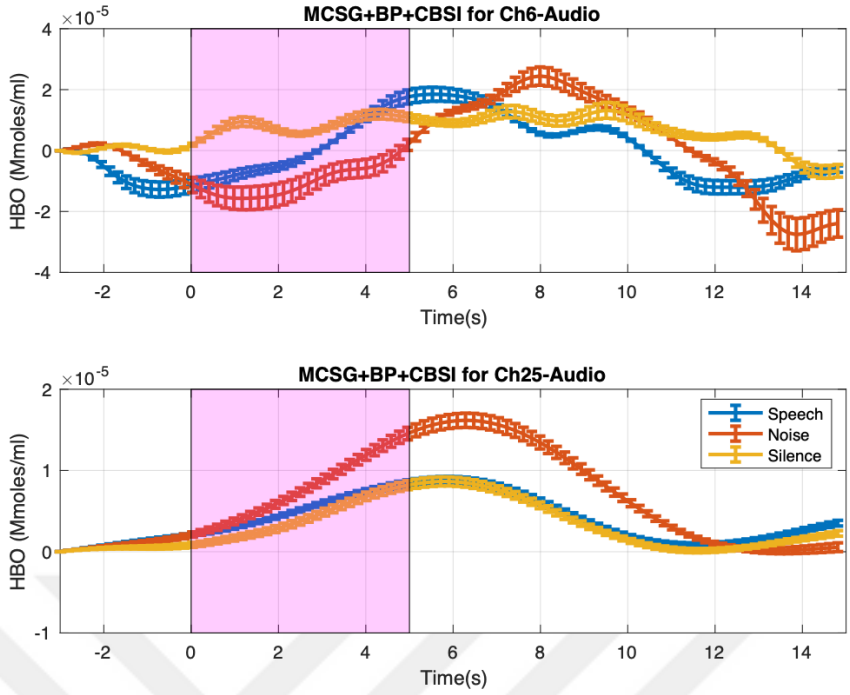

Figure 5.3. Block Average result of Method 2 (MCSG + BP + CBSI) for Channel 6 and Channel 25

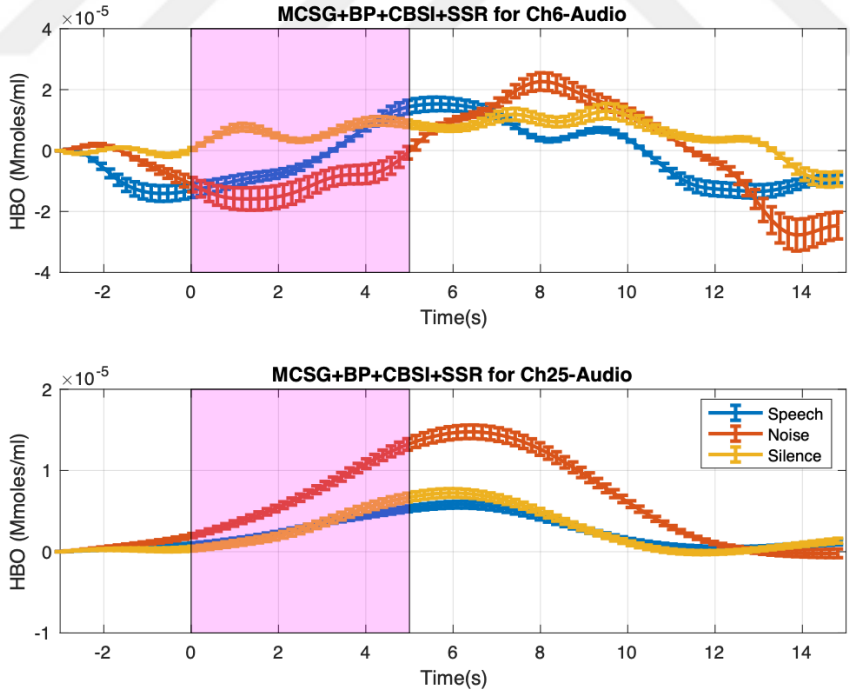

Figure 5.4. Block Average result of Method 3 (MCSG + BP + CBSI + SS) for Channel 6 and Channel 25

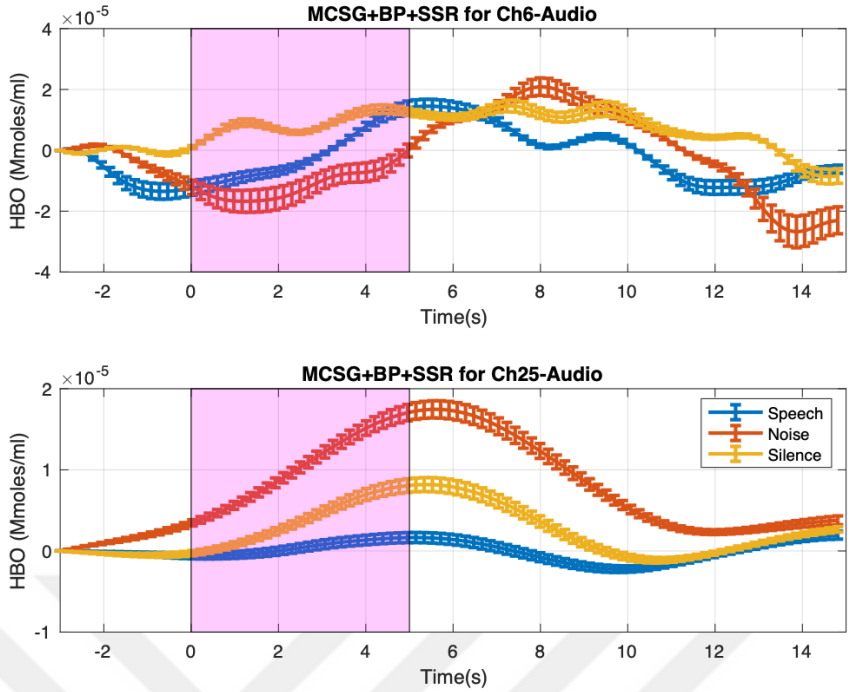

Figure 5.5. Block Average result of Method 4 (MCSG + BP + SS) for Channel 6 and Channel 25

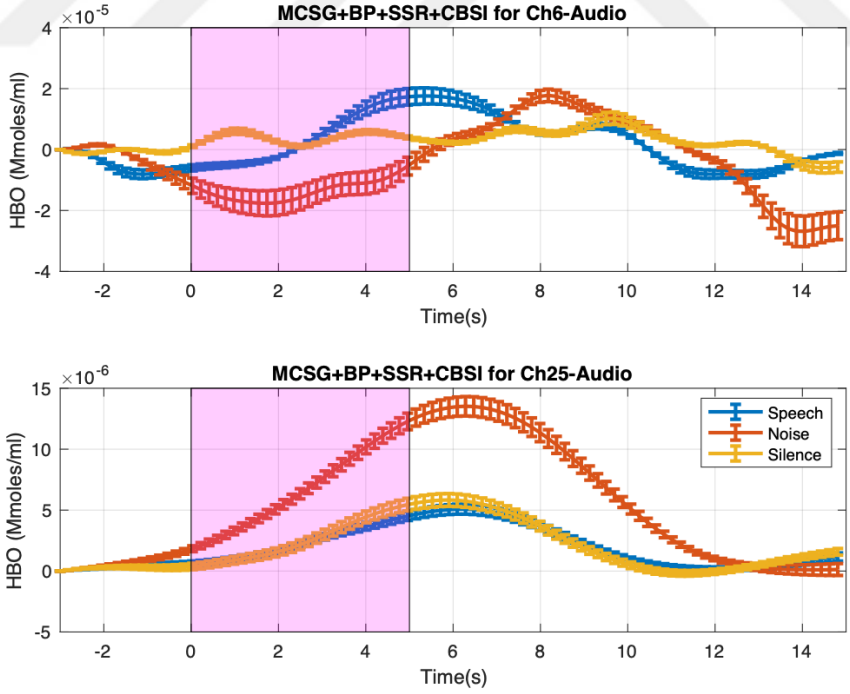

Figure 5.6. Block Average result of Method 5 (MCSG + BP + SS + CBSI) for Channel 6 and Channel 25

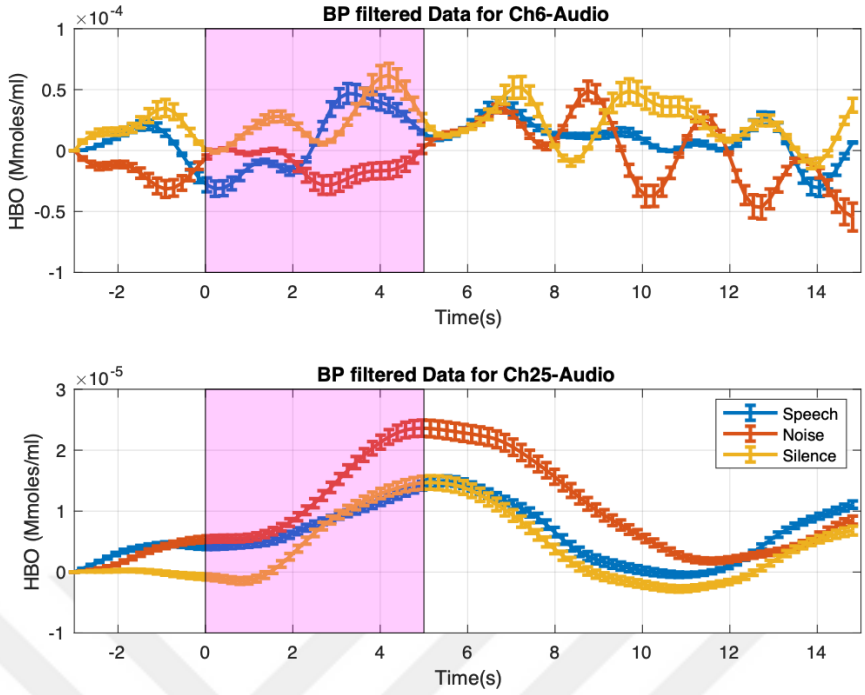

Figure 5.7. Block Average result of Method 6 (BP Only) for Channel 6 and Channel 25

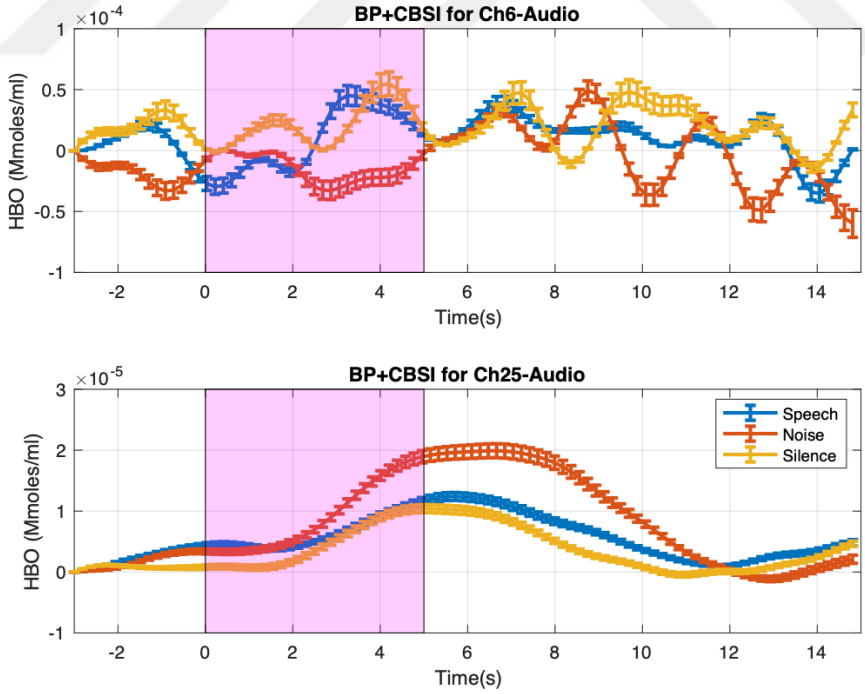

Figure 5.8. Block Average result of Method 7 (BP + CBSI) for Channel 6 and Channel 25

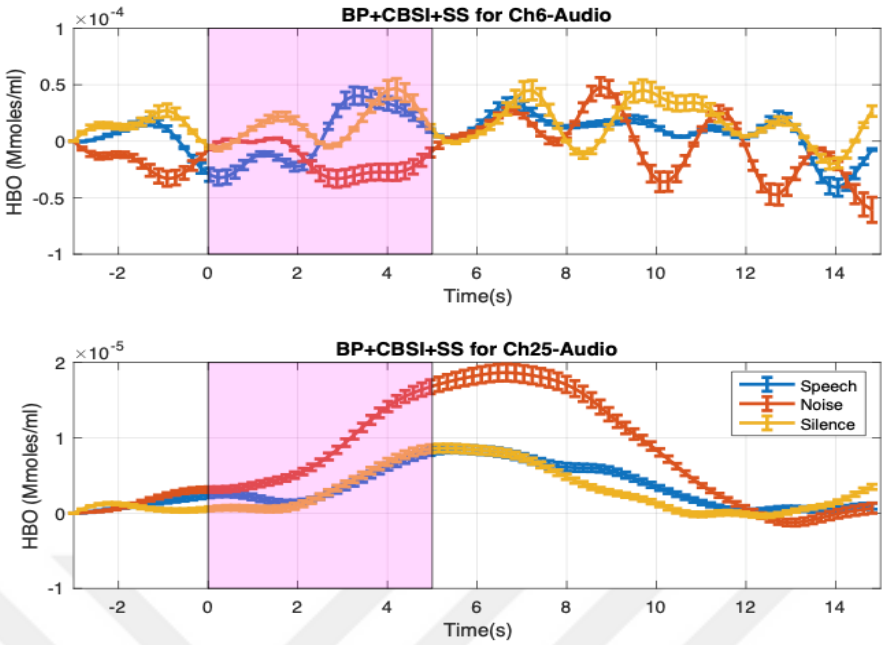

Figure 5.9. Block Average result of Method 8 (BP + CBSI + SS) for Channel 6 and Channel 25

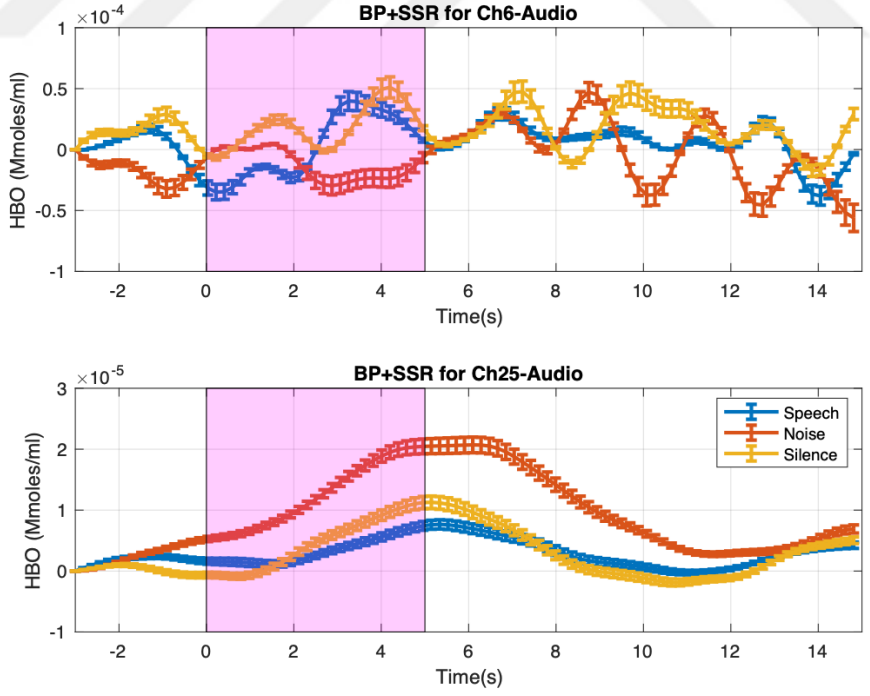

Figure 5.10. Block Average result of Method 9 (BP + SS) for Channel 6 and Channel 25

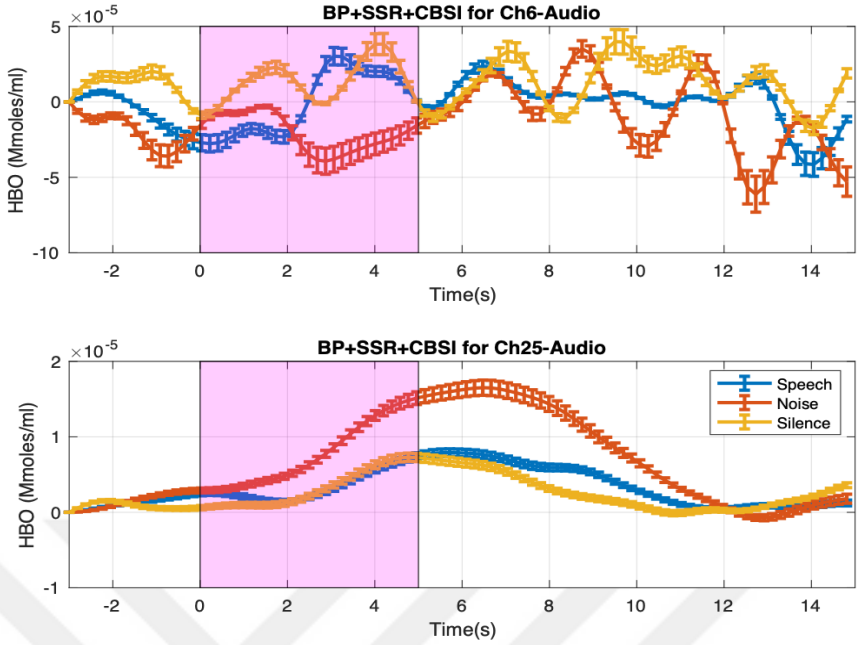

Figure 5.11. Block Average result of Method 10 (BP + SS + CBSI) for Channel 6 and Channel 25

All figures between Figure 5.2. to Figure 5.11. demonstrate the impact of each method on channels 6 and 25. The observation of substantial differences in waveforms resulting from distinct preprocessing pipelines deserves considerable attention. This phenomenon underscores the noteworthy impact that various preprocessing approaches can have on the shape and characteristics of recorded waveforms in experimental data. The variations in waveforms across different preprocessing strategies illuminate the intricate interplay between data processing steps and the subsequent patterns of neural activity revealed by the analyses.

Method	Stim 1, Ch 6	Stim 1, Ch 25
M1 (MCSG+BP)	2,74	0
M2 (MCSG+BP+CBSI)	3,38	3,28
M3 (MCSG+BP+CBSI+SS)	0	2,26
M4 (MCSG+BP+SS)	0	0
M5 (MCSG+BP+SS+CBSI)	0	0
M6 (BP ONLY)	2,40	2,87
M7 (BP+CBSI)	3,69	3,52
M8 (BP+CBSI+SS)	2,52	2,81
M9 (BP+SS)	0	0
M10 (BP+SS+CBSI)	2,68	3,08

Table 5.3. T-values of all methods for Stimulus 1 (Speech)

Method	Stim 2, Ch 6	Stim 2, Ch 25
M1 (MCSG+BP)	0	3,45
M2 (MCSG+BP+CBSI)	3,10	4,09
M3 (MCSG+BP+CBSI+SS)	2,87	4,31
M4 (MCSG+BP+SS)	2,12	3,79
M5 (MCSG+BP+SS+CBSI)	2,40	4,19
M6 (BP ONLY)	2,42	3,35
M7 (BP+CBSI)	2,87	4,36
M8 (BP+CBSI+SS)	2,53	4,64
M9 (BP+SS)	2,27	3,26
M10 (BP+SS+CBSI)	0	4,36

Table 5.4. T-values of all methods for Stimulus 2 (Noise)

Table 5.3. shows the t-values for Channel 6 and Channel 25 for stimuli 1 (Speech). Also, Table 5.4. shows the t-values for Channel 6 and Channel 25 for stimuli 2 (Noise). Table 5.5. demonstrates average performance of these 4 groups for all of the 10 methods.

A high t-value indicates that the mean of CNR values obtained for that channel data over all participants is statistically significantly different than zero. This suggests that the observed difference from 0 is likely not due to random chance alone and we can claim with over 95 % confidence that the mean CNR values are significantly different than 0. A high t-value is often associated with a low p-value, indicating that there is strong evidence against the null hypothesis which is in our case 'Mean of CNR values obtained across all participants CNR values is zero for that channel when fNIRS signals are preprocessed with that method specific pipeline'. The null hypothesis is rejected in favor of the alternative hypothesis in channel data when the probability of accepting the null hypothesis is below the calculated p value.

Method	Average Performance
M1 (MCSG+BP)	1,54
M2 (MCSG+BP+CBSI)	3,46
M3 (MCSG+BP+CBSI+SS)	2,36
M4 (MCSG+BP+SS)	1,47
M5 (MCSG+BP+SS+CBSI)	1,65
M6 (BP ONLY)	2,76
M7 (BP+CBSI)	3,61
M8 (BP+CBSI+SS)	3,12
M9 (BP+SS)	1,38
M10 (BP+SS+CBSI)	2,53

Table 5.5. Average performance of t-values for each method (CH6 and CH25)

Table 5.5. provides useful information to specify the best method. When we compare the average performances of t-values for each method for our regions of interest (ROI), the method which has the highest t score is determined as Method 7 (Bandpass Filter + Correlation Based Signal Improvement). The second best method is Method 2 (Motion Correction Spline SG + Bandpass Filter + Correlation Based Signal Improvement). Methods with the worst performance are Method 9 (Bandpass Filter + Short Separation Regression) and Method 4 (Motion Correction Spline SG + Bandpass Filter + Short Separation Regression).

Therefore, the best method is Method 7 and the worst method is Method 9.

6. CONCLUSION

The ultimate aim of this study was to compare the performance of various preprocessing pipelines for proposing the best solution to the noise problem and reducing the motion artifacts in long channel fNIRS signals by use of short channel information.

Over the course of the past ten years, a multitude of diverse techniques aimed at denoising and correcting motion artifacts in FNIRS data have been explored with the objective of enhancing the quality of recorded signals. Despite these efforts, a universally accepted and definitive method has not yet emerged as the standard choice for the majority of research groups. Various digital filtering approaches proved insufficient in effectively eliminating noise elements, while conversely, other methods exhibited the potential to inadvertently diminish the strength of the activation signal. This lack of consensus underscores the ongoing challenges in establishing a robust approach to denoising and motion correction in the realm of FNIRS studies. In this study, we examined at how different noise removal strategies affect the signal quality of audio fNIRS data. We aimed to find the best combination of preprocessing steps for fNIRS measurements when the channels are placed close together. We compared the efficacy of these filters in recovering hemodynamic activation in expected regions of interest that covered mainly the bilateral Heschl's Gyri. Our goal was to figure out the method that would increase hemodynamic response quality in terms of the CNR metric. For this purpose, we implemented 10 different preprocessing methodologies. These methods included motion correction spline SG, short channel regression, bandpass filter and correlation-based signal improvement. We used Homer3 functions while implementing these methods.

In future research endeavors, further exploration and refinement of noise reduction techniques, motion artifact correction methods, and data analysis approaches will be crucial in advancing the reliability and accuracy of fNIRS studies conducted with short channel separation. Additionally, the integration of advanced machine learning algorithms and real-time processing capabilities holds the potential to revolutionize the field, enabling real-time artifact identification and adaptive correction strategies.

7. REFERENCES

1. Zhang, F., Cheong, D., Khan, A. F., Chen, Y., Ding, L., & Yuan, H. (2021, August). Correcting physiological noise in whole-head functional near-infrared spectroscopy. Journal of Neuroscience Methods, 360, 109262. https://doi.org/10.1016/j.jneumeth.2021.109262

2. Kirilina, E., Jelzow, A., Heine, A., Niessing, M., Wabnitz, H., Brühl, R., Ittermann, B., Jacobs, A. M., & Tachtsidis, I. (2012, May). The physiological origin of task-evoked systemic artefacts in functional near infrared spectroscopy. *NeuroImage*, *61*(1), 70–81. https://doi.org/10.1016/j.neuroimage.2012.02.074

3. Pinti, P., Tachtsidis, I., Hamilton, A., Hirsch, J., Aichelburg, C., Gilbert, S., & Burgess, P. W. (2020, March). The present and future use of functional near-infrared spectroscopy (fNIRS) for cognitive neuroscience. Annals of the New York Academy of Sciences, 1464(1), 5–29. https://doi.org/10.1111/nyas.13948

4. Nguyen, H. D., Yoo, S. H., Bhutta, M. R., & Hong, K. S. (2018, December). Adaptive filtering of physiological noises in fNIRS data. BioMedical Engineering OnLine, 17(1). https://doi.org/10.1186/s12938-018-0613-2

5. Rayi, A., & Murr, N. (2022). Electroencephalogram. In *StatPearls*. StatPearls Publishing.

6. Zhang, Y., Wang, K., Wei, Y., Guo, X., Wen, J., & Luo, Y. (2022). Minimal EEG channel selection for depression detection with connectivity features during sleep. *Computers in biology and medicine*, *147*, 105690. https://doi.org/10.1016/j.compbiomed.2022.105690

7. A XUE, G., CHEN, C., LU, Z. L., & DONG, Q. (2010, February 3). Brain Imaging Techniques and Their Applications in Decision-Making Research. *Acta Psychologica Sinica*, *42*(1), 120–137. https://doi.org/10.3724/sp.j.1041.2010.00120

8. Uğurbil K. (2012). Development of functional imaging in the human brain (fMRI); the University of Minnesota experience. *NeuroImage*, *62*(2), 613–619. https://doi.org/10.1016/j.neuroimage.2012.01.13

9. Cohen D. (1972). Magnetoencephalography: detection of the brain's electrical activity with a superconducting magnetometer. *Science (New York, N.Y.), 175*(4022), 664–666. https://doi.org/10.1126/science.175.4022.664

10. Cohen D. (1968). Magnetoencephalography: evidence of magnetic fields produced by alpha-rhythm currents. *Science (New York, N.Y.), 161*(3843), 784–786. https://doi.org/10.1126/science.161.3843.784

11. Kao, C., & Zhang, Y. (2019). Magnetic Source Imaging and Infant MEG: Current Trends and Technical Advances. *Brain sciences*, *9*(8), 181. https://doi.org/10.3390/brainsci9080181

12. Baillet S. (2017). Magnetoencephalography for brain electrophysiology and imaging. Nature neuroscience, 20(3), 327–339. https://doi.org/10.1038/nn.4504

13. Catana C. (2019). Development of Dedicated Brain PET Imaging Devices: Recent Advances and Future Perspectives. Journal of nuclear medicine : official publication, Society of Nuclear Medicine, 60(8), 1044–1052. https://doi.org/10.2967/jnumed.118.217901

14. Rahman, M. A., Siddik, A. B., Ghosh, T. K., Khanam, F., & Ahmad, M. (2020, September 28). A Narrative Review on Clinical Applications of fNIRS. *Journal of Digital Imaging*, *33*(5), 1167–1184. https://doi.org/10.1007/s10278-020-00387-1

15. Ferrari, M., & Quaresima, V. (2012, November). A brief review on the history of human functional near-infrared spectroscopy (fNIRS) development and fields of application. *NeuroImage*, *63*(2), 921–935. https://doi.org/10.1016/j.neuroimage.2012.03.049

16. Scholkmann, F., Kleiser, S., Metz, A. J., Zimmermann, R., Mata Pavia, J., Wolf, U., & Wolf, M. (2014, January). A review on continuous wave functional near-

infrared spectroscopy and imaging instrumentation and methodology. *NeuroImage*, *85*, 6–27. https://doi.org/10.1016/j.neuroimage.2013.05.004

17. Yücel, M. A., Lühmann, A. V., Scholkmann, F., Gervain, J., Dan, I., Ayaz, H., Boas, D., Cooper, R. J., Culver, J., Elwell, C. E., Eggebrecht, A., Franceschini, M. A., Grova, C., Homae, F., Lesage, F., Obrig, H., Tachtsidis, I., Tak, S., Tong, Y., . . . Wolf, M. (2021, January 7). Best practices for fNIRS publications. *Neurophotonics*, *8*(01). https://doi.org/10.1117/1.nph.8.1.012101

18. Boas, D. A., Gaudette, T., Strangman, G., Cheng, X., Marota, J. J., & Mandeville, J. B. (2001, January). The Accuracy of Near Infrared Spectroscopy and Imaging during Focal Changes in Cerebral Hemodynamics. NeuroImage, 13(1), 76–90. https://doi.org/10.1006/nimg.2000.0674

19. Kim, M., Lee, S., Dan, I., & Tak, S. (2022, February 1). A deep convolutional neural network for estimating hemodynamic response function with reduction of motion artifacts in fNIRS. Journal of Neural Engineering, 19(1), 016017. https://doi.org/10.1088/1741-2552/ac4bfc

20. Sappia, M. S., Hakimi, N., Colier, W. N. J. M., & Horschig, J. M. (2020, October 27). Signal quality index: an algorithm for quantitative assessment of functional near infrared spectroscopy signal quality. Biomedical Optics Express, 11(11), 6732. https://doi.org/10.1364/boe.409317

21. Sutoko, S., Chan, Y. L., Obata, A., Sato, H., Maki, A., Numata, T., Funane, T., Atsumori, H., Kiguchi, M., Tang, T. B., Li, Y., Frederick, B. D., & Tong, Y. (2019, January 9). Denoising of neuronal signal from mixed systemic low-frequency oscillation using peripheral measurement as noise regressor in near-infrared imaging. Neurophotonics, 6(01), 1. https://doi.org/10.1117/1.nph.6.1.015001

22. Hocke, L., Oni, I., Duszynski, C., Corrigan, A., Frederick, B., & Dunn, J. (2018, May 8). Automated Processing of fNIRS Data—A Visual Guide to the Pitfalls and Consequences. Algorithms, 11(5), 67. https://doi.org/10.3390/a11050067

23. Jahani, S., Setarehdan, S. K., Boas, D. A., & Yücel, M. A. (2018, February 8). Motion artifact detection and correction in functional near-infrared spectroscopy: a new hybrid method based on spline interpolation method and Savitzky–Golay filtering. Neurophotonics, 5(01), 1. https://doi.org/10.1117/1.nph.5.1.015003

24. Cooper, R. J., Selb, J., Gagnon, L., Phillip, D., Schytz, H. W., Iversen, H. K., Ashina, M., & Boas, D. A. (2012). A Systematic Comparison of Motion Artifact Correction Techniques for Functional Near-Infrared Spectroscopy. Frontiers in Neuroscience, 6. https://doi.org/10.3389/fnins.2012.00147

25. Scholkmann, F., Spichtig, S., Muehlemann, T., & Wolf, M. (2010, March 22). How to detect and reduce movement artifacts in near-infrared imaging using moving standard deviation and spline interpolation. Physiological Measurement, 31(5), 649–662. https://doi.org/10.1088/0967-3334/31/5/004

26. A Brigadoi, S., Ceccherini, L., Cutini, S., Scarpa, F., Scatturin, P., Selb, J., Gagnon, L., Boas, D. A., & Cooper, R. J. (2014, January). Motion artifacts in functional near-infrared spectroscopy: A comparison of motion correction techniques applied to real cognitive data. *NeuroImage*, 85, 181–191. https://doi.org/10.1016/j.neuroimage.2013.04.082

27. Hu, X. S., Hong, K. S., & Ge, S. S. (2011, October). Recognition of stimulus-evoked neuronal optical response by identifying chaos levels of near-infrared spectroscopy time series. *Neuroscience Letters*, *504*(2), 115–120. https://doi.org/10.1016/j.neulet.2011.09.011

28. Naseer, N., & Hong, K. S. (2015, January 28). fNIRS-based brain-computer interfaces: a review. *Frontiers in Human Neuroscience*, *9*. https://doi.org/10.3389/fnhum.2015.00003

29. Yücel, M. A., Selb, J., Aasted, C. M., Petkov, M. P., Becerra, L., Borsook, D., & Boas, D. A. (2015, September 11). Short separation regression improves statistical significance and better localizes the hemodynamic response obtained by near-infrared spectroscopy for tasks with differing autonomic responses. *Neurophotonics*, *2*(3), 035005. https://doi.org/10.1117/1.nph.2.3.035005

30. Luke, R., Larson, E., Shader, M. J., Innes-Brown, H., Van Yper, L., Lee, A. K. C., Sowman, P. F., & McAlpine, D. (2021). Analysis methods for measuring passive auditory fNIRS responses generated by a block-design paradigm. Neurophotonics, 8(2),025008. https://doi.org/10.1117/1.NPh.8.2.02500